

**Appendix B: Benchmark Analysis with CFAST and
FDS, Monideep DEY, NRC/NIST, USA**

SUMMARY

This Appendix presents analyses conducted with the CFAST and FDS fire models for an international benchmark exercise aimed at evaluating the capability of current fire models to simulate cable tray fires of redundant safety systems in nuclear power plants. The exercise involved simulating fire scenarios in a large nuclear power plant compartment with cable trays as targets in varying ventilation conditions. The analyses demonstrate that both the CFAST and FDS codes provide a treatment of most physical phenomena in the scenarios analyzed. The predicted time scale and magnitude of the main parameters of interest in these scenarios by both codes are similar. The sub-model for the target, and issues regarding the thermal environment of the target, are the largest source of uncertainty for these types of scenarios. It will be useful to conduct validation exercises for CFAST and FDS in which the predictive capability of target damage is the main focus of the validation. These exercises will provide information to allow the development of quantitative estimates of the uncertainties for the major parameters of interest.

INTRODUCTION

The analysis presented in this Appendix was conducted as part of a benchmark exercise in the International Collaborative Project to Evaluate Fire Models for Nuclear Power Plant Applications (Dey, 2000). The objective of the collaborative project is to share the knowledge and resources of various organizations to evaluate and improve the state of the art of fire models for use in nuclear power plant fire safety and fire hazard analysis. The project is divided into two phases. The objective of the first phase is to evaluate the capabilities of current fire models for fire safety analysis in nuclear power plants. The second phase will implement beneficial improvements to current fire models that are identified in the first phase, and extend the validation database of those models. Currently, twenty-two organizations from six countries are represented in the collaborative project.

The first task of the international collaborative project is to evaluate the capability of fire models to analyze cable tray fires of redundant safety systems in nuclear power plants. The safety systems are required to safely shutdown the reactor during abnormal and emergency events in the plant. A specified distance separates cable trays of redundant safety systems if they are located in the same compartment in which a single fire could potentially damage both systems. Therefore, the analysis of fires that could damage redundant safety trains is an important part of nuclear power plant fire hazard analysis. The evaluation of the capability of fire models to analyze these scenarios is being conducted through an international benchmark exercise.

The benchmark exercise (Bertrand and Dey, 2001) is intended to simulate a basic scenario defined in sufficient detail to allow evaluation of the physics modeled in the fire computer codes. An assessment of appropriate input parameters and assumptions, interpretation of results, and determining the adequacy of the physical sub-models in the codes for specific scenarios will establish useful technical information regarding the capabilities and limitations of the fire computer codes. This valuable information will be documented in a technical reference manual for fire model users. Generic insights regarding the capabilities of the models will also be developed in this process and documented. The comparisons between codes can be used to understand the modeling of the physics in them, i.e. if all the codes

produce similar results over a range of scenarios then the physics modeled in the codes is probably adequate for this scenario. However, the compounding effects of different phenomena will also need to be examined as part of this evaluation. Some variations in the results may be acceptable depending on how the results will be used. Uncertainties in the predictions based on validations of each code will provide a basis for the confidence on the set of results developed in the exercise.

This Appendix presents the analyses for the benchmark exercise conducted using the Consolidated Fire And Smoke Transport [CFAST] (Jones, 2000), and Fire Dynamic Simulator [FDS] (McGrattan, 2000) computer codes developed by the National Institute of Standards and Technology, U.S. Department of Commerce. The paper provides the results of an assessment and verification of the capability of these computer codes to analyze the fire scenario specified for the benchmark exercise.

DEFINITION OF SCENARIO

A representative emergency switchgear room for a Pressurized Water Reactor (PWR) has been selected for this benchmark exercise. The room is 15.2 m (50 ft) deep x 9.1 m (30 ft) wide and 4.6 m (15 ft) high. The room contains the power and instrumentation cables for the pumps and valves associated with redundant safety systems. The power and instrument cable trays run the entire depth of the room, and are separated horizontally by a distance, d . The cable trays are 0.6 m (≈ 24 in) wide and 0.08 m (≈ 3 in) deep. A simplified schematic of the room, illustrating critical cable tray locations, is shown in Figure 1. The room has a door, 2.4 m x 2.4 m (8 ft x 8 ft), and a mechanical ventilation system with a flow rate of 5 volume changes per hour in and out of the room.

There are two parts to the exercise. The objective of Part I is to determine the maximum horizontal distance between a specified transient (trash bag) fire and tray A that results in the ignition of tray A. Part II examines whether the target cable tray B will be damaged for several heat release rates of the cable tray stack (A, C2, and C1), and horizontal distance, d . The effects of the fire door being open or closed, and the mechanical ventilation on or off, are examined in both parts of the benchmark exercise.

VALIDATION OF THE CFAST AND FDS FIRE CODES

The CFAST and FDS fire codes have been compared to several data sets from experiments, including those with configurations and fire intensities similar to that specified for the benchmark exercise. However, none of the tests included cable trays as target material to measure the response of the target to the physical environment in the compartment.

Results from the CFAST code have been compared to several tests of fires in spaces ranging from small compartments to large aircraft hangers. Peacock (1993) compared predictions of CFAST to four fire tests in a single compartment, multi-compartment on a single floor, and a seven-story building. The magnitude and trends (time to critical conditions and general curve shape) are reported. The comparisons ranged from a few percent to a factor of 2 to 3 of the measured values.

Results from the FDS code, Version 1, has been compared with experimental data for open plumes, back draft, flashover, a warehouse fire, pool fires in a Navy Hangar, and fires in a decommissioned nuclear reactor containment. These comparisons demonstrated the enhanced predictive capability of this code for a wide range of fire scenarios, and also identified areas for improvement. Specifically, the modeling of radiation from the hot gases and walls is an important effect in nuclear power plant compartment fires. The modeling of this effect has been included in Version 2, which was released in December 2001. Significant improvements in the predictions of the tests in the decommissioned containment building have been achieved with FDS, Version 2.

Although several comparisons of these codes to experimental data are available, it is not possible at this stage to translate this research to quantitative estimates of uncertainties of the predicted results from the codes for the benchmark exercise. A complete analysis of past validation research, including an examination of the effect of the specifics (compartment configuration, fire source intensity, ventilation, etc.) of a fire scenario on the predictive capability of the codes is planned.

RESULTS OF THE ANALYSES

Part I

CFAST Analyses

The major sub-models used in CFAST for the scenarios specified in the benchmark exercise are (1) combustion chemistry (tracking O_2 , and species); (2) plumes and layers; (3) vent flow, including forced ventilation; and (4) heat transfer, especially radiation and convection to the target.

The following presents the major highlights of the results obtained for the analysis of the benchmark exercise. The trends of various parameters are examined to verify the adequacy of the basic sub-models for the specific scenarios. The general conclusions from the exercise are also presented, although as indicated above, quantitative estimates of the uncertainties associated with the predictive capability of the codes for the specific parameters examined are not available at this time.

The measured heat release rate (Lee, 1985) of a large trash bag was used as input for the simulation as shown in Figure 2. In order to conduct a simplified and conservative analysis, the target is assumed to be a single power cable with a diameter of 50 mm at the bottom left corner of the cable tray A. Consistent with the target models in CFAST and FDS, the target cable is represented as a rectangular slab oriented horizontally with a thickness of 50 mm. The cable is assumed to ignite when the centerline of the cable reaches 643 K. Table 1 summarizes the cases for Part I of the benchmark exercise. The peak heat release for the trash bag fire (Figure 2) for Part I is ≈ 350 kW, and peaks at ≈ 150 s.

Table 1. Summary of Cases for Part I

	<u>Distance between Trash Bag & Cable</u>	<u>Door</u>	<u>Ventilation System</u>
Base Case	2.2 m	Closed*	Off
Case 1	0.3 ⁺		
Case 2	0.9		
Case 3	1.5		
Case 4		Open	
Case 5			On

* For simulations with the door closed, a crack (2.4 m x 0.005 m) at the bottom of the doorway was assumed.

⁺A value in a cell indicates the parameter was varied from the base case.

Base Case

Figure 3 shows the predicted oxygen depletion for the Base Case. The oxygen concentration in the lower layer stays approximately constant, as would be expected. The oxygen concentration in the upper layer decreases by $\approx 1\%$ to 19.2%. Therefore, the fire will not be limited by oxygen in this fire scenario.

Figure 2 also shows the plume flow development during this scenario. The main plume flow increases rapidly at the initiation of the fire, and does not follow the fire heat release rate, as expected. CFAST over predicts mass entrainment at the initial stages of the fire because of the plume height used in the calculation of the entrained air. Initially, the plume height is assumed to be from the fire to the ceiling. This leads to an over prediction of the initial mass flow to the upper layer, and the rate of descent of the gas layer interface.

Figure 4 shows the hot gas layer (HGL) temperature and the interface height development. The upper layer temperature peaks at ≈ 230 s, about 80 s after the fire peaks, due to the lag time for the heating of the gas by the fire. In this scenario, the upper layer temperature increases only about 50 K. After peaking, the upper layer temperature decreases with time due to the heat loss to the boundaries. The interface height decreases rapidly initially due to high plume flow (see Figure 2). The rate of descent of the interface height decreases after ≈ 230 s when the HGL temperature has peaked. The hot gas layer is prevented from reaching the floor due to air inflow at the crack below the door caused by a negative pressure in the compartment (see Figure 5).

Figure 5 shows the pressure development, and the resulting flows in and out of the compartment. The pressure peaks at ≈ 150 s when the fire heat release rate peaks, as would be expected. The pressure decreases after the fire peaks due to outflow from the compartment at the crack under the door, and swings to a negative value. The small oscillations in the pressure after ≈ 250 s is due to the small fluctuations in the heat release rate. The peak in the outflow is consistent with the pressure profile, and the outflow goes to zero when the pressure in the compartment is less than the outside. The initiation of inflow is consistent with the pressure profile, and is much less than the outflow. The small oscillation of the inflow is caused by the fluctuations in the pressure.

Figure 6 shows the components of the heat flux to the target. The radiative flux on the target from the fire follows the fire heat release rate curve, as expected. The radiative flux on the target (lower side) from the hot gas increases at the point (≈ 100 s) when the interface height reaches the target. The radiative flux from the hot gas on the target peaks at ≈ 280 s, 50 s after the upper layer temperature peaks, and decreases in a similar manner to the upper layer temperature. The lag between the peak in the radiative flux from the hot gas and the upper layer temperature is because of the time needed for hot gas layer growth under the target. The convective flux is negative initially because the target temperature is greater than the lower layer temperature. The convective flux becomes positive and starts to increase at ≈ 100 s when the hot gas layer interface reaches the target, as expected. The convective flux peaks at ≈ 230 s when the upper layer temperature peaks, as expected.

Cases 1 to 3

Figure 7 shows the target surface temperatures versus time for the Base Case and Cases 1 -3. For the Base Case, the target temperature peaks at ≈ 290 s, ≈ 140 s after the fire and target flux reaches its peak due to the thermal inertia of the target. The target surface temperature only increases ≈ 20 K for this case. Figure 8 is a plot of the maximum surface temperatures of the target versus the distance between the fire and target. The plot could be approximated by a straight line and does not show a rapid increase in temperature with decreasing distance between the fire and the target. This can be explained by examining Case 1. The radiative flux from the hot gas layer is the same as the Base Case since the only difference between the cases is the fire location. The radiation from the fire is the largest in Case 1 because the fire is closest to the target; however, the peak convective flux is half of that in the Base Case (100 vs. 200 W/m^2). The decreased peak convective flux is caused by a smaller difference in temperature between the hot gas layer and the target surface (the target surface temperature is higher due to higher radiative flux).

Cases 4 and 5

The following presents some key features of the results of Case 4 and 5. Figure 9 shows the development of the interface height for Case 4 versus the Base Case. The interface height approaches a constant value at ≈ 140 s, after the HGL reaches the top of the door at ≈ 100 s. Figure 10 shows the development of the upper layer outflow and lower layer inflow after the HGL interface reaches the door at ≈ 100 s, indicating the establishment of a neutral plane below the top of the door (at ≈ 2.2 m). Figure 11 shows the HGL temperature development for Case 4 and 5. The HGL temperature for Case 4 is less than the Base Case after ≈ 270 s because of the outflow of hot gas from the upper layer (which reaches its peak value at ≈ 200 s) through the door, and higher plume flow. The HGL temperature for Case 5 is less than that in the Base Case after ≈ 100 s when the HGL reaches the mechanical vents, and ambient air is injected into and hot gas ejected from the hot gas layer.

Figure 12 shows the development of flows in the mechanical ventilation system for Case 5. The transitions in flows from the mechanical vents in and out of the gas layers occurs at about ≈ 100 s when the HGL reaches the mechanical vents. The mass flow rate into the upper layer is larger than the mass flow rate out of the upper layer because mechanical

ventilation flows in CFAST are specified as volumetric flow rates. The temperature of the flow out of the compartment is higher than the ambient conditions of the flow into the compartment. Figure 3 shows that the oxygen concentration in the HGL layer is greater in Case 5 than the Base Case after ≈ 160 s when the HGL reaches the mechanical vents, and air at ambient conditions is injected in to the upper layer. Figure 7 shows the target surface temperature for Case 4 and 5 along with the other cases. The target surface temperature for Case 4 and 5 is less than in the Base Case because of cooler hot gas layer temperatures. The cable temperature does not approach the point of ignition (643 K) in any of the cases analyzed.

The above analyses of the results for Part 1 demonstrates that CFAST provides a treatment of most physical phenomena of interest in the scenarios analyzed. The results indicate that the trends predicted by the sub-models in CFAST are reasonable and provide insights beneficial for nuclear power plant fire safety engineering.

FDS Analyses

The following presents a summary of the analyses that was conducted with the FDS code in order to allow a comparison with the results from CFAST. Direct comparison between CFAST and FDS for several parameters discussed above is difficult. The total flow through vents is not a direct output from the FDS code. Plume flow and the hot gas layer interface height are computed directly in a zone model, but not in CFD models.

Figure 13 is an output image from the Smokeview (Forney, 2000) graphical interface to the FDS code, which allows a comprehensive visual analysis of the code output. The specific image in Figure 13 is a slice file, which shows the development of system parameters versus time for a particular plane in the 3-D geometry simulated. This specific figure shows a snapshot of the temperature profile at the midpoint of the room (where the trash bag is located) for the Base Case at 230 s. Although it is not possible to obtain an accurate determination of the interface height from images such as shown in Figure 13, a visual examination of the slice file versus time showed that the time scales for hot gas layer development and peak temperatures (at ≈ 230 s for the Base Case, Case 4, and Case 5) predicted by CFAST and FDS are similar. Similar observations of the pressure slice file simulations indicated that the magnitude and timing of the pressure peak (at ≈ 150 s for the Base Case) were also similar.

Figure 14 is a vector plot of temperature in a plane parallel to the cable trays at the midpoint of the room (and door) and illustrates the flow patterns for Case 4 in which the door is open. Outflow and inflow at the door around the neutral plane is illustrated, as also predicted by the CFAST code. Figure 15 is a similar plot in a plane perpendicular to the cable trays at the midpoint of the room (and fire) and illustrates the flow patterns caused by the mechanical ventilation system in Case 5. This information will be necessary to examine the local effects of target heating.

One important difference in the results from the CFAST and FDS codes for the type of scenarios examined for the Benchmark Exercise is the hot gas temperature. CFAST, a two-zone code, calculates the *average* temperature of the hot gas layer, whereas FDS computes the entire temperature profile in the compartment. The peak average HGL temperature (at \approx

275 s) predicted by CFAST for the Base Case is 77 C. The temperature profile predicted by FDS for this case (at ≈ 275 s) ranged from 75 C in the lower region to 130 C in the upper region of the hot gas. This temperature gradient in the hot gas will determine the convective heat flux to the cable tray depending on its vertical position. Table 2 compares the results obtained from the CFAST and FDS codes. Most of the results are similar. The largest difference is noted for the convective heat flux to the target in the Base Case. This is expected because the vertical temperature gradient would be the largest for this case with no ventilation. The differences in the target surface temperatures calculated for all the cases analyzed are within 20 %.

Table 2. Comparison of CFAST and FDS Results

	Max. Rad. Flux (w/m ²) At Target		Max. Conv. Flux (w/m ²) At Target		Max. Target Surface Temp. (K)	
	CFAST	FDS	CFAST	FDS	CFAST	FDS
Base Case	587	712	188	485	322	333
Case 4	582	704	186	277	321	325
Case 5	588	710	148	180	318	319

Part II

The following presents the results of analyses with the CFAST code. Due to time constraints, FDS was not exercised for Part II of the benchmark Exercise.

Predicting the heat release rate of a burning cable tray stack is extremely complex, therefore, the mass loss rate of the burning cable tray stack was defined as input in the exercise. The consecutive ignition and burning of all 3 cable trays (trays A, C2, and C1) were modeled as one fire. The analyses were conducted assuming a peak heat release rate for the whole cable tray stack between 1 – 3 MW. A t-squared fire growth with $t_0 = 10$ min., and $Q_0 = 1$ MW was assumed, where:

$$Q=Q_0 (t/t_0)^2$$

The cable fire was assumed to last for 60 minutes at the peak heat release rate, and decay in a t-squared manner with similar constants as for growth.

The heat source (trays A, C2, and C1) was assumed to be at the center of the cable tray length and width and at the same elevation as the bottom of tray C2. The target (representing tray B) was assumed to be at the center of the cable tray length. In order to conduct a simplified and conservative analysis, the target was assumed to be a single power or instrumentation cable, without an electrical conductor inside the cable, and with a diameter of 50 mm or 15 mm respectively at the bottom right corner of cable tray B. The target in CFAST is modeled as a rectangular slab, and was assumed to be horizontally oriented with a thickness of 50 mm or 15 mm. The cable was assumed to be damaged when the centerline of the cable reached 473 K.

Table 3 summarizes the cases for Part II of the benchmark exercise.

Table 3 Summary of Cases for Part II

Fire Scenario	HRR (MW)	D (m)	Door Position	Mech. Vent. Sys.	Target	Target Elev. (m)
Base Case	1	6.1	Closed*	Off	Power Cable	1.1
Case 1		3.1 ⁺				
Case 2		4.6				
Case 3	2	3.1				
Case 4	2	4.6				
Case 5	2	6.1				
Case 6	3	3.1				
Case 7	3	4.6				
Case 8	3	6.1				
Case 9			Open>15 min	Off>15 min		
Case 10			Open	On		
Case 11						2.0
Case 12						Same
Case 13					Instrument Cable	

* For simulations with the door closed, a crack (2.4 m x 0.005 m) at the bottom of the doorway was assumed.

⁺A value in a cell indicates the parameter is varied from the base case.

Base Case

Figures 16 to 20 show the predicted results of the main parameters of interest. Figure 21 shows the pyrolysis rate specified for the case. The predicted trend for the heat release rate, interface height, and oxygen concentration in Figures 16, 17, and 18 is collectively examined. CFAST predicts that the HGL interface lowers to the fire source (at an elevation of 3.4 m) at ≈ 580 s. The heat release rate decreases rapidly at this time since the oxygen concentration in the HGL is lower than the specified lower oxygen limit of 12 %. The interface height increases at this point due to inflow into the lower layer from the outside caused by a rapid reduction in the heat release rate and pressure. The heat release rate increases after this point due to the fluctuations in the interface height that temporarily expose the fire source to sufficient oxygen in the lower layer. After ≈ 600 s, the interface height starts to decrease slowly as a result of continued pyrolysis and the production of hydrocarbons.

The HGL profile shown in Figure 19 is consistent with the HRR profile shown in Figure 16. The HGL temperature reaches its peak of ≈ 440 K at ≈ 600 s when the HRR peaks, and decreases rapidly with the heat release rate. The HGL approaches ambient conditions at ≈ 1200 s shortly after the HRR goes to zero. The target surface temperature is shown in Figure 20 and peaks at ≈ 600 s at a value 323 K, only 23 K above ambient conditions. The target temperature then decreases at a less rapid rate than the HGL temperature due to the thermal inertia of the PVC cable.



The above analysis demonstrates the complexity in modeling an elevated fire source which can be affected by a limited oxygen environment. The assumption for the LOL will have a significant effect on the predicted peak target temperature. Conservative assumptions are warranted due to the uncertainty in the extinction model used in CFAST.

Cases 1 and 2

Analysis of the results for Cases 1 and 2 showed that the distance between the fire and target did not have a strong effect on the target temperature. The absence of the typical strong effect of the distance between the fire and target due to the radiative flux incident on the target was discussed earlier.

Cases 3 to 8

As discussed above, the cable tray fire in the Base Case is limited by the oxygen depletion in the environment. Cable tray fires that could be potentially more intense (as specified by the pyrolysis rate for these cases) are also limited, i.e., the HRRs are similar to that specified for the Base Case. Therefore, these cases are not discussed further here.

Special Case

Since the fire was extinguished after ≈ 720 s and well before 4800 s, the expected duration of the fire, a special case was analyzed. The special case was the same as the Base Case, except the fire was located at an elevation below the top of the door at 1.8 m, and the door was open. Natural ventilation of the hot gases through the door prevented the HGL from reaching and extinguishing the cable tray fire. Therefore, a fire that was sustained at the specified intensity for 3600 s was achieved. Figure 22 shows the HGL and target surface temperature development. The HGL and target surface temperatures peaked at 457 K and 435 K.

CONCLUSIONS

The above analyses of the benchmark exercise for cable tray fires of redundant safety systems demonstrate that both the CFAST and FDS codes provide a treatment of most physical phenomena in the scenarios analyzed. For Part I, the time scale and magnitude of the development of the main parameters of interest in these scenarios are similar. The difference in the predicted target surface temperature between the codes is less than 20 % for the scenarios analyzed. Comparisons of these results with those obtained by others using different fire codes in the benchmark exercise will further verify the physical sub-models in these codes. Comparison of code results with data from a test series specifically focused on target damage would broaden the validation database of these codes.

The analysis of the scenarios in Part II demonstrate the complexity in modeling an elevated fire source that can be affected by a limited oxygen environment. The extinction sub-models utilized in CFAST is an approximation of the interaction of the complex combustion process with a limited oxygen environment. Therefore, the result from the extinction sub-model represents an approximation of the conditions expected for the fire scenarios. The assumption for the LOL will affect the predicted peak target temperature. Therefore, conservative assumptions are warranted due to the uncertainty in the extinction model.

It is concluded that the results obtained from these codes can provide insights beneficial for nuclear power plant fire safety analysis for the type of scenarios analyzed, if the limitations of the code is understood. Further analyses of different fire scenarios are planned. The sub-model for the target, and issues regarding the thermal environment of the target, are the largest source of uncertainty for the types of scenarios in Part I. It will be useful to conduct validation exercises for CFAST and FDS in which the predictive capability of target damage is the main focus of the validation. Also, more refined measurements and data analyses are needed to estimate the quantitative uncertainties of the parameters predicted in the analyses of these fire scenarios. The code results, with quantitative estimates of the uncertainties in the predicted parameters, should provide a sound basis for engineering judgments in nuclear power plant fire safety analysis.

REFERENCES

Dey, M.K., "International Collaborative Project to Evaluate Fire Models for Nuclear Power Plant Applications: Summary of Planning Meeting," NUREG/CP-0170, U.S. Nuclear Regulatory Commission, Washington, DC, April 2000.

Bertrand, R, and Dey, M.K., "International Collaborative Project to Evaluate Fire Models for Nuclear Power Plant Applications: Summary of 2nd Meeting," NUREG/CP-0173, U.S. Nuclear Regulatory Commission, Washington, DC, July 2001.

Floyd, J., "Comparison of CFAST and FDS for Fire Simulation with the HDR T51 and T52 Tests," NISTIR 6866, National Institute of Standards and Technology, Gaithersburg, Maryland, April 2002.

Forney, G.P., and McGrattan, K.B., "User's Guide for Smokeview Version 1.0 – A Tool for Visualizing Fire Dynamics Simulation Data," NISTIR 6513, National Institute of Standards and Technology, Gaithersburg, Maryland, May 2000.

Jones, W.W., Forney, G.P., Peacock, R.D., and Reneke, P.A., "A Technical Reference for CFAST: An Engineering Tool for Estimating Fire and Smoke Transport," NIST TN 1431, National Institute of Standards and Technology, Gaithersburg, Maryland, January 2000.

Lee, B. T., "Heat Release Rate Characteristics of Some Combustible Fuel Sources in Nuclear Power Plants," NBSIR 85-3195, National Bureau of Standards, 1985.

McGrattan, K.B., Baum, H.R., Rehm, R.G., Hamins, A., & Forney, G.P., "Fire Dynamics Simulator - Technical Reference Guide," NISTIR 6467, National Institute of Standards and Technology, Gaithersburg, Maryland, January 2000.

Peacock, R.D., W.W. Jones, and R.W. Bukowski, "Verification of a Model of Fire and Smoke Transport," *Fire Safety Journal*, Vol. 21, pp. 89–129, 1993.

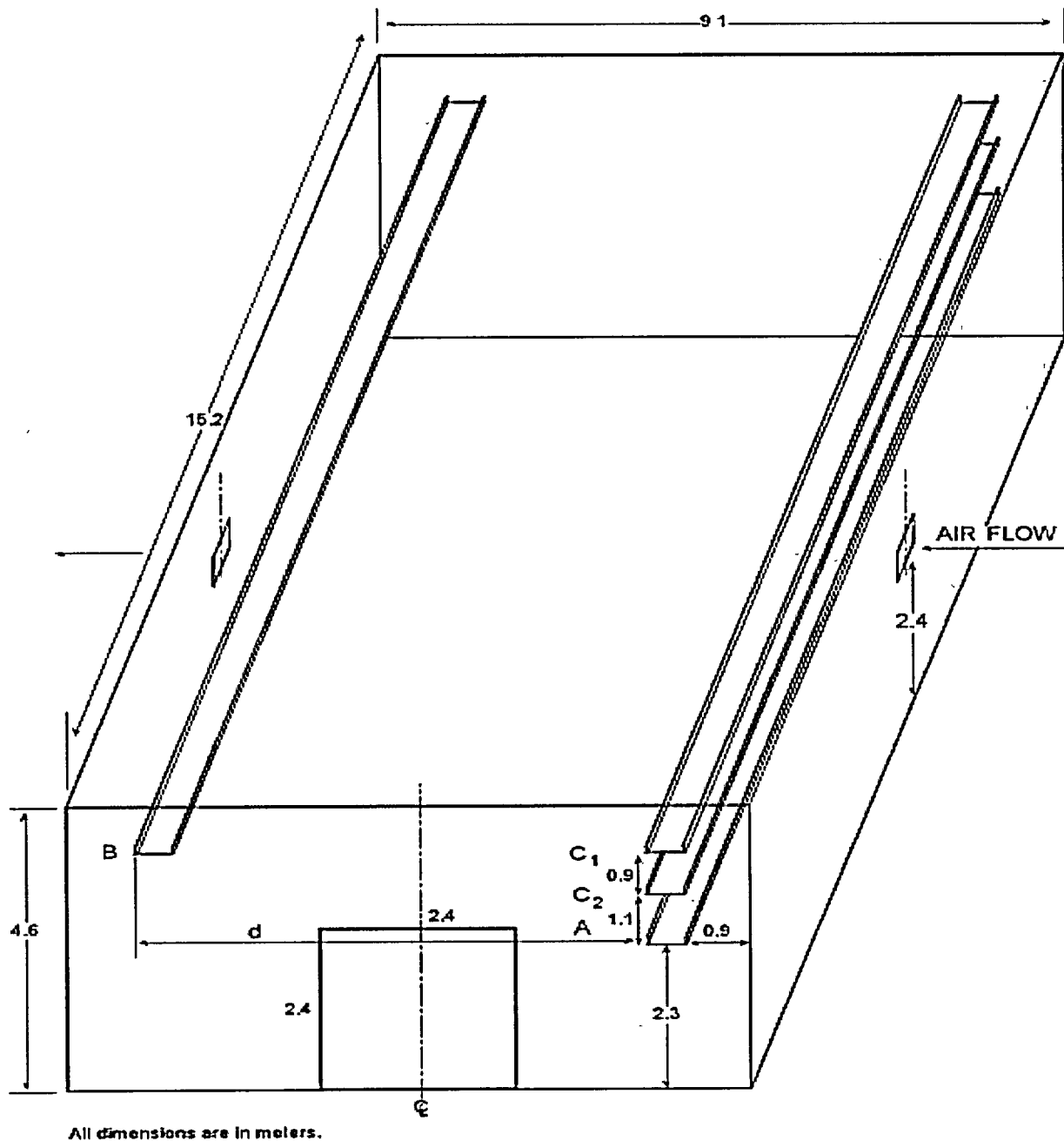


Figure 1 Schematic of PWR Room

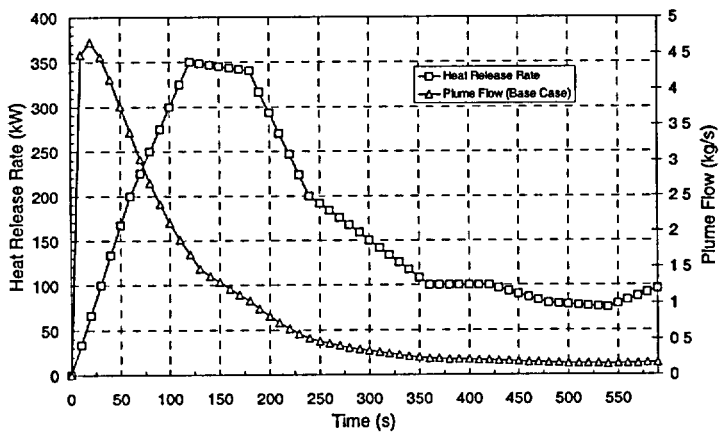


Figure 2 Heat Release Rate and Plume Flow-B-12

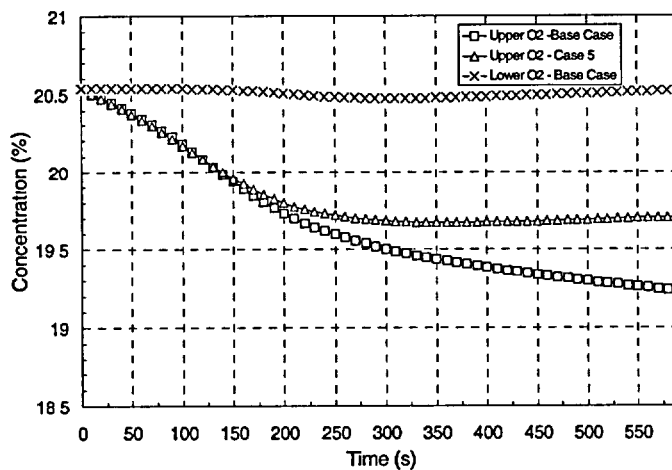


Figure 3 Oxygen Concentrations - Part I

1-1

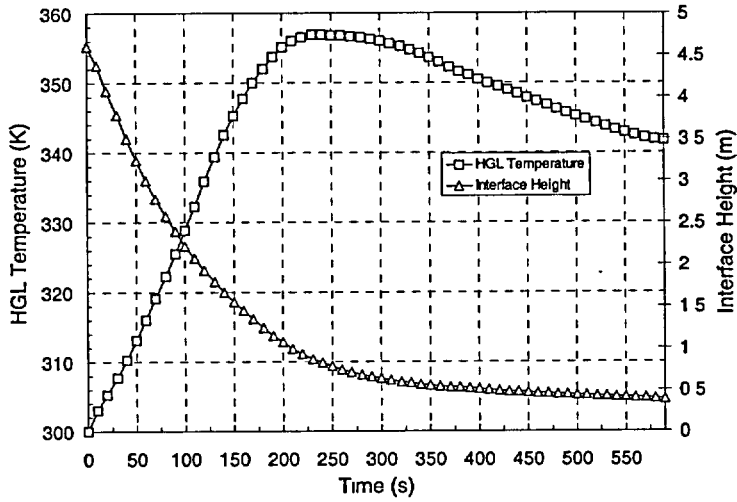


Figure 4 HGL Development
- Base Case, Part I

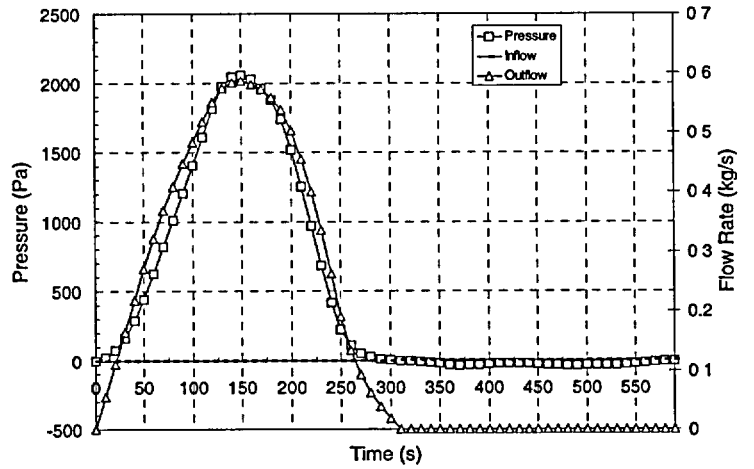


Figure 5 Pressure and Vent Flow Development
- Base Case, Part I

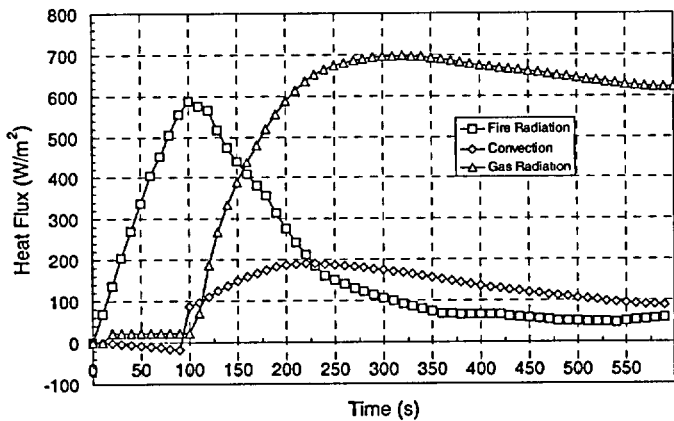


Figure 6 Heat Fluxes - Base Case, Part I

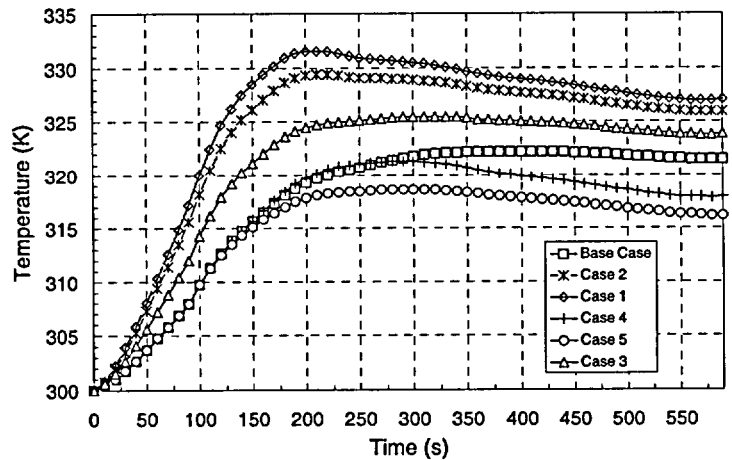


Figure 7 Target Surface Temperatures,
Part I

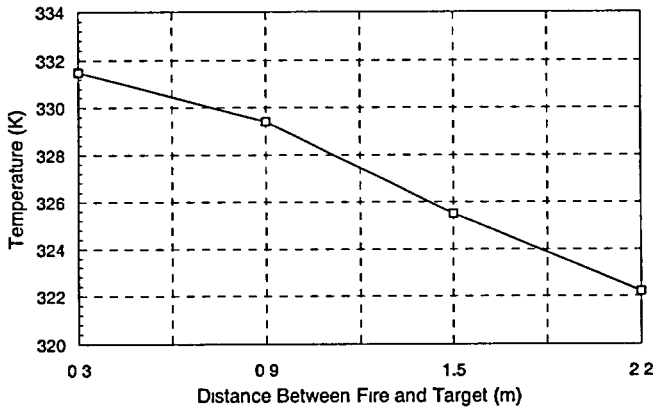


Figure 8 Target Surface Temperatures, Part I

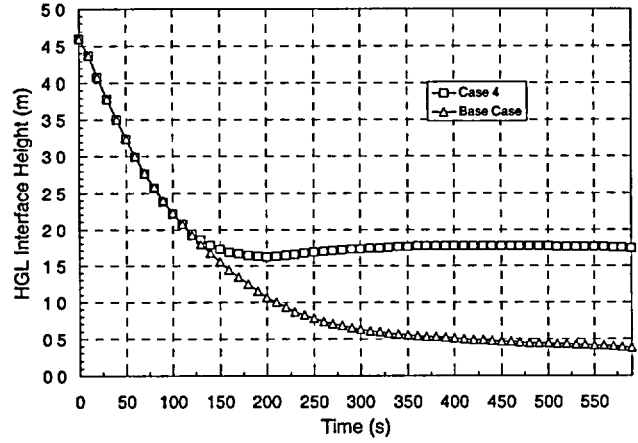


Figure 9 HGL Development - Case 4, Part I

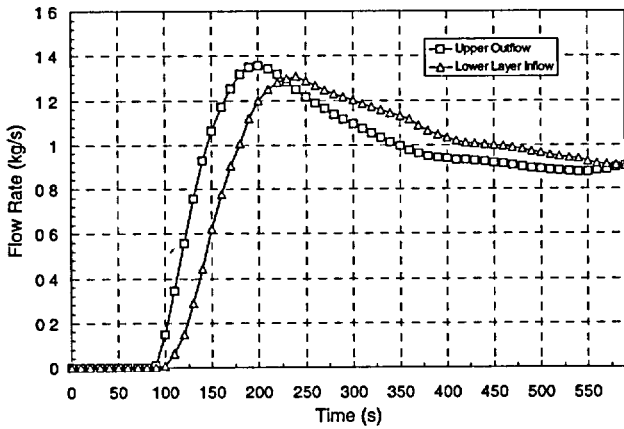


Figure 10 Door Flows - Case 4, Part I

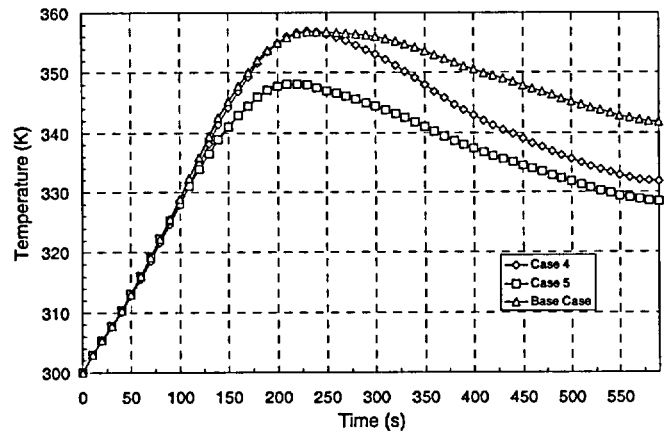


Figure 11 HGL Temperature, Part I

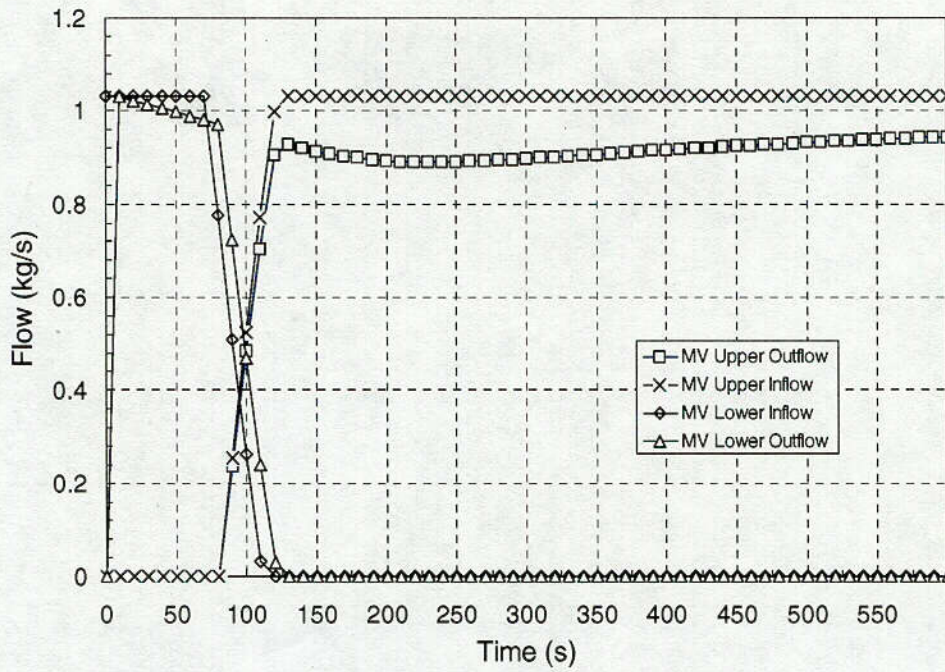


Figure 12 Mechanical Ventilation Flows – Case 5, Part I

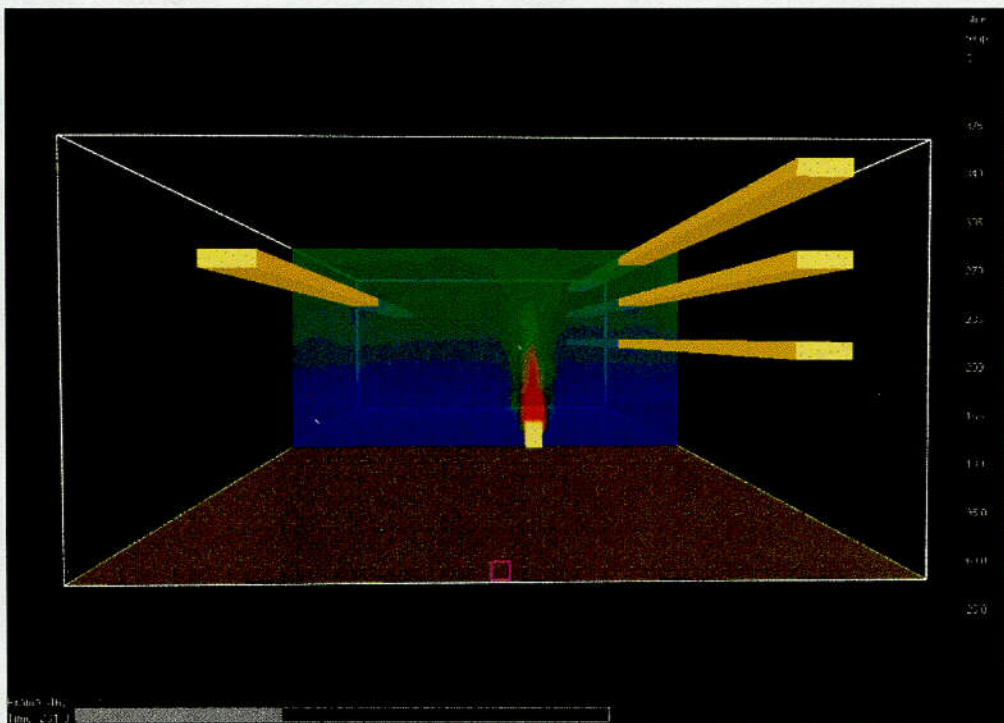


Figure 13 Temperature Profile – Base Case, Part I at 230 s

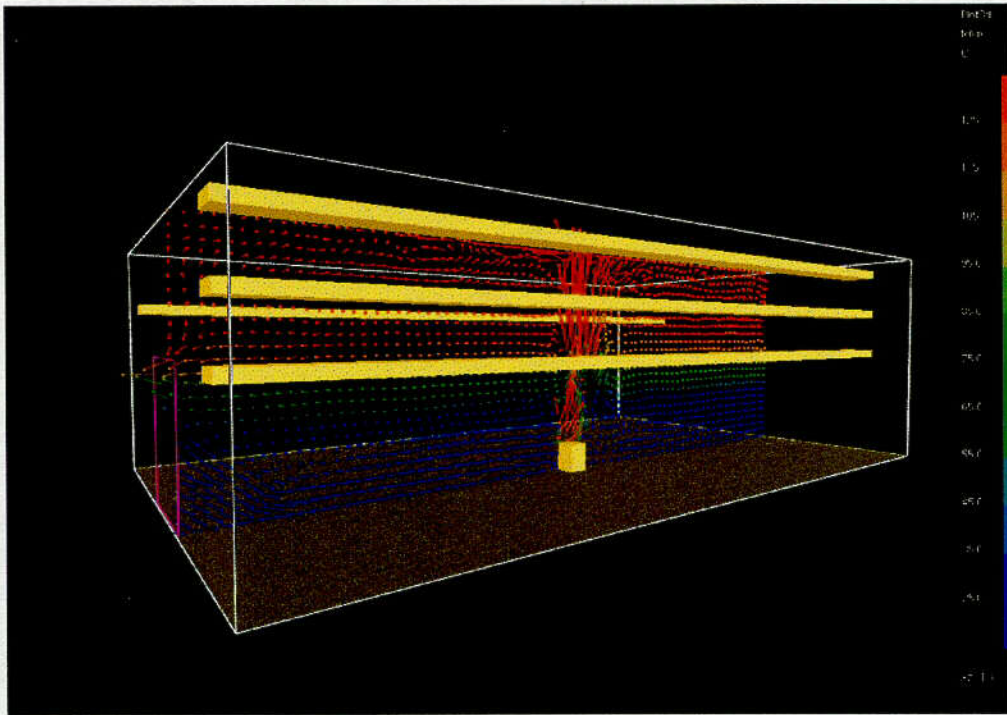


Figure 14 Door Flows – Case 4, Part I

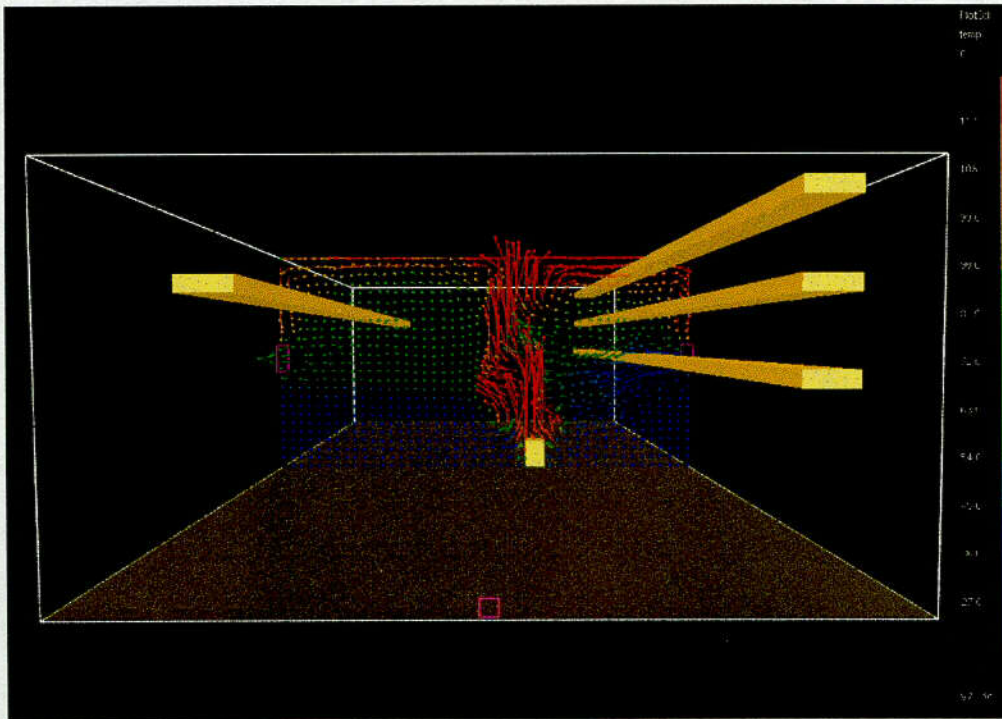


Figure 15 Effects of Mechanical Ventilation –Case 5, Part I

CO2
138

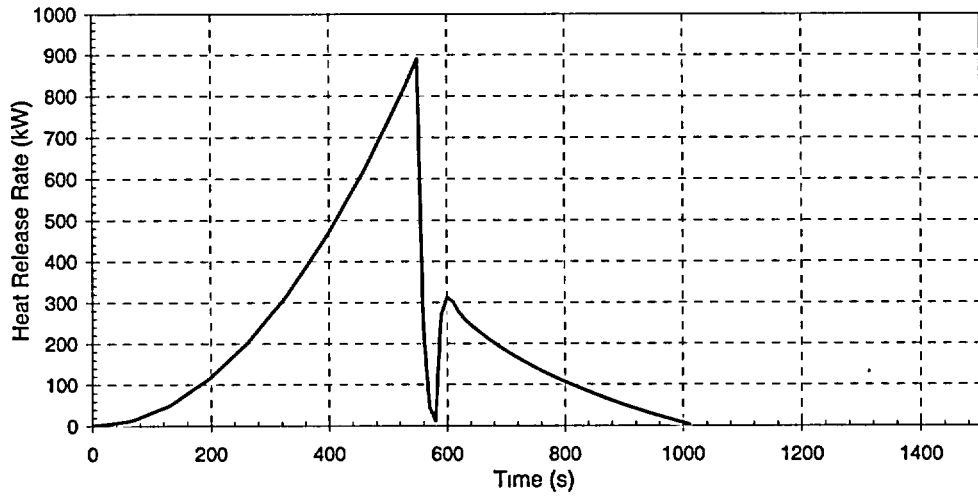


Figure 16 Heat Release Rate, Base Case, Part II

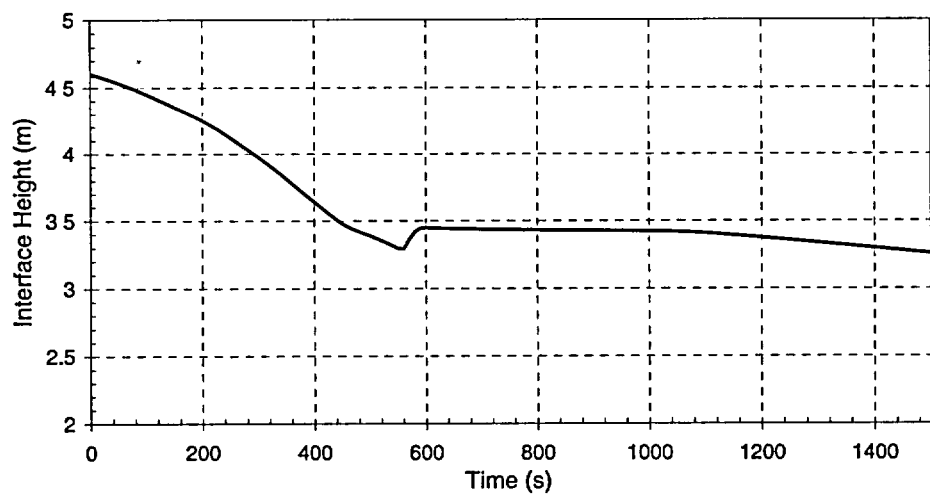


Figure 17 Interface Height, Base Case, Part II

121

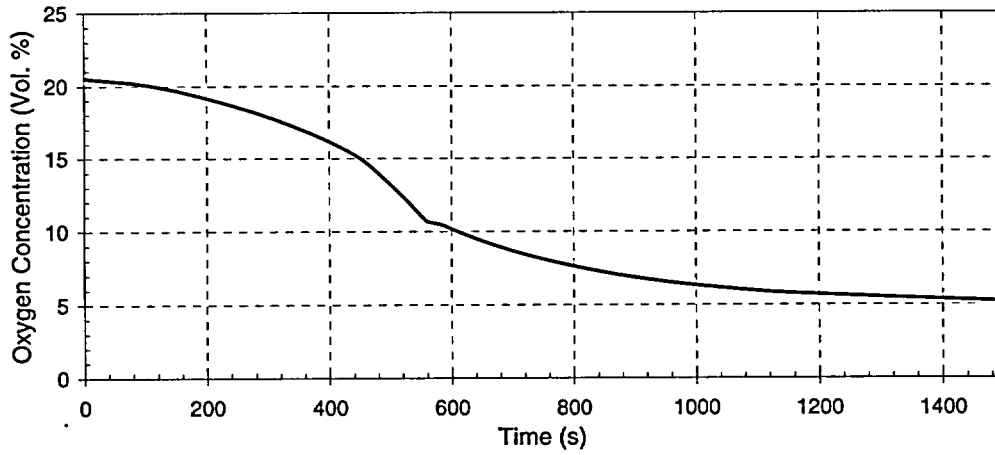


Figure 18 Oxygen Concentration, Base Case, Part II

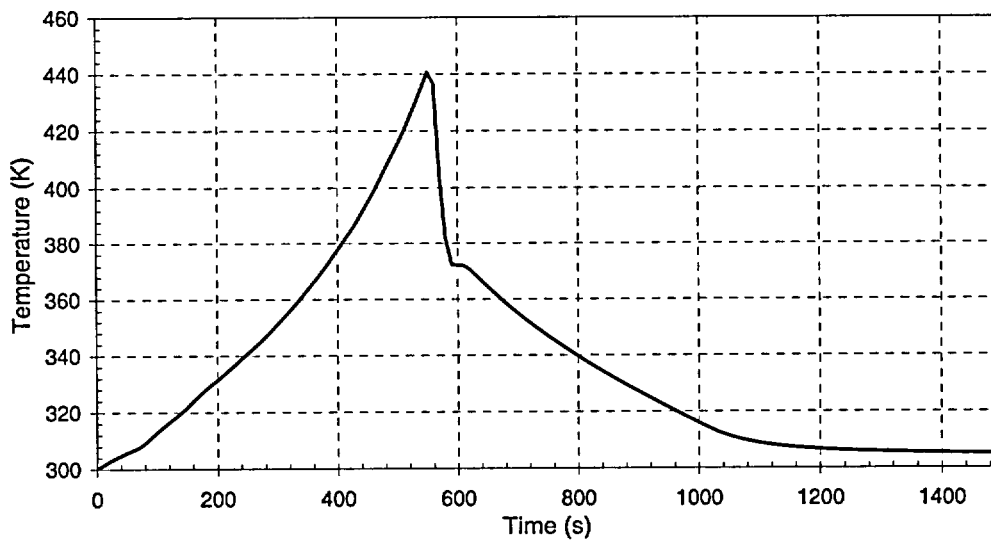


Figure 19 HGL Temperature, Base Case, Part II

Handwritten mark

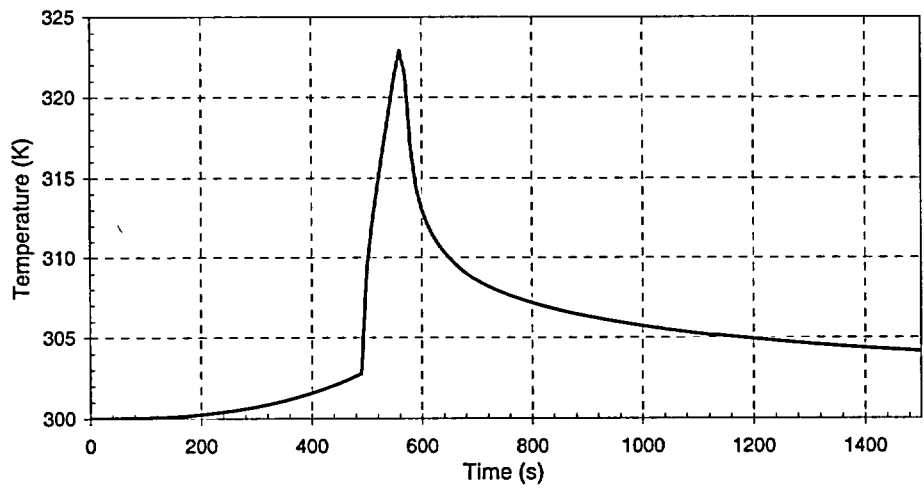


Figure 20 Target Surface Temperature, Base Case, Part II

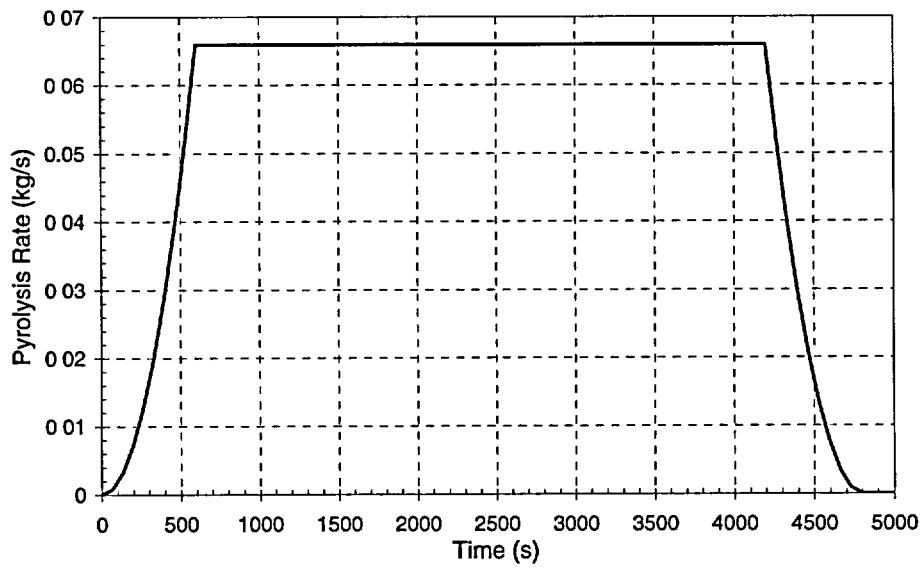


Figure 21 Pyrolysis Rate, Base Case, Part II

191

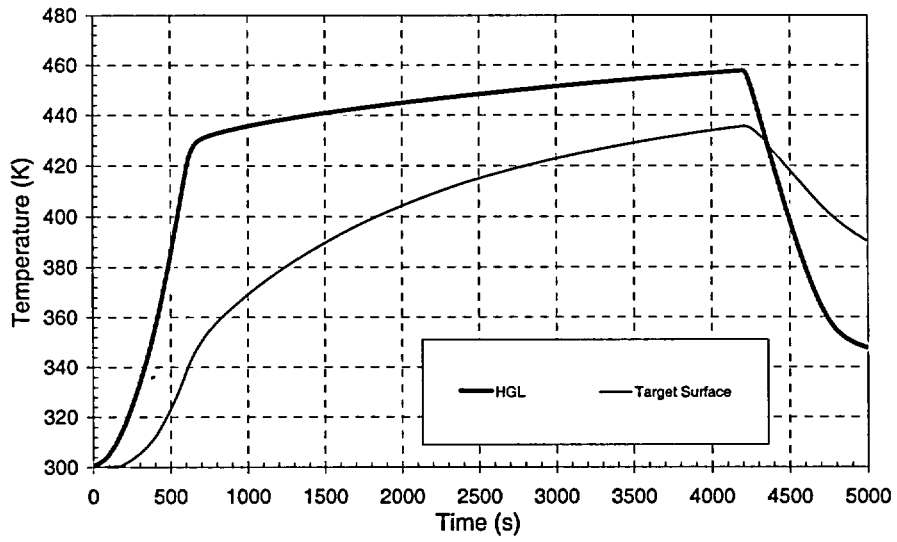


Figure 22 Temperature Development, Special Case, Part II

(15)

**Appendix C: Benchmark Analysis with MAGIC,
Bernard GAUTIER, Helene ERNANDORENA, and
Maurice KAERCHER, EdF, France**

International Collaborative Project to Evaluate Fire Models for
Nuclear Power Plant Applications
Benchmark Exercise # 1
Cable Tray Fires of Redundant Safety Trains

Simulation of a single room problem using code MAGIC

Bernard GAUTIER - H el ene ERNANDORENA
EDF R&D 6 quai Watier 78401 Chatou FRANCE
Maurice KAERCHER
EDF SEPTEN 12-14 Avenue Dutrievoz 69628 Villeurbanne FRANCE

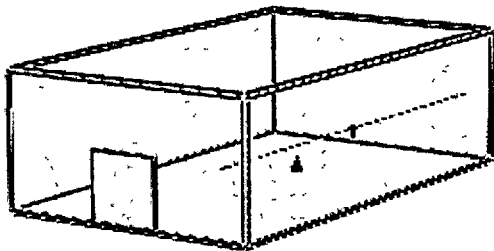
Introduction

The calculations presented here were done with MAGIC V 3.4.7. The code was used in its standard version. MAGIC uses a two-zone model including most of the classic features:

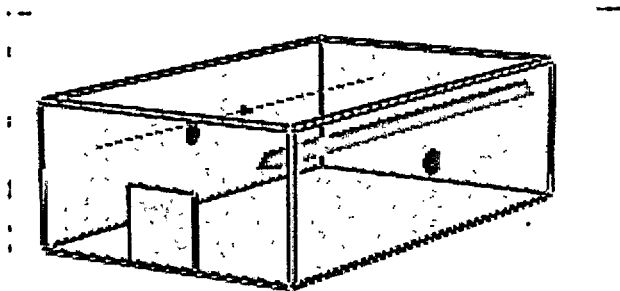
- Gaseous phase combustion, governed by pyrolysis rate, product properties and oxygen feeding (plume entrainment)
- Two homogeneous smoke and gas layer temperature and concentration stratification, mass and energy balances into gases
- Heat transfers by contact and radiation between flame, gases and smoke, walls and surrounding air, thermal conduction in multi-layer walls, obstacles to radiation
- Mass flow transfer: Fire-plumes, ceiling-jet, openings and vents
- Thermal behavior of targets and cables, secondary source ignition, unburnt gas flames across opening

A data base for combustibles and materials is also available. A description of the code features can be obtained in [1]. The validation file of the code [2] is based on full-scale experiment data. This file is used to improve the validated range of the code: volumes from 11 to 1300 m³, fires from 100kW to 2.5 MW, mono-compartment and multi-compartment varied configurations, liquid fires, solid fires, pool fires, linear fires

Two case were proposed to the participants (figure 1 - [4]). Simulation were done with Version 3.4.7 of MAGIC with a LOL (Low Oxygen Limit) of 12%, then of 0%.



Part 1: fluxes on a target exposed to a bag fire (5 cases studied)



Part 2: redundant tray B exposed to a trash tray A cable fire (13 cases studied)

Figure 1 : the proposed cases

114

Input parameters

The data used for input was directly provided by the benchmark definition of scenario [4].

Some of the requested parameters were not taken into account :

- the wall emissivity (0.94 wanted) is fixed to 0.9 in MAGIC
- air humidity (Magic considers dry air)
- the door structure is not considered in MAGIC (adiabatic material)
- the specie yields are not considered in MAGIC. Only $[O_2]$, $[C_nH_m]$ and smoke properties are considered in MAGIC, their production is obtained from the source and plume behavior.
- chemical characteristics of cables were not taken into account: only thermo-physical characteristics are necessary in MAGIC.
- the tray width and depth were not necessary : we use a single cable to obtain a conservative approach of the cable temperature increase.

Some missing data which had to be set:

- smoke opacity for the trash-bag fire was fixed to 0.5 m^{-1}
- the missing stoichiometric ratio for the trash-bag fire was fixed to $1.184 \text{ gO}_2/\text{g}$

Some other data was not fixed by the text and let to the user choice :

- wall effect on plume : this option impacts on the plume correlation, using a mirror effect when the plume is confined to a wall.
 - the conduction meshing is not automated in version 3.4.7. The user is supposed to apply the Fourier Law in order to mesh correctly. This last point is one of the most current user effects observed on the code. The meshing is automated and optimized from version 3.4.8.
- Least, the time step and the end of simulation time were not specified in [4].

Part I : result analysis

Base case:

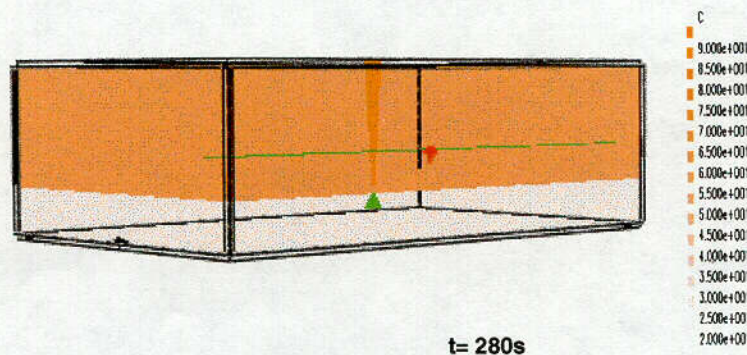


figure1: part I base Case : smoke filling of the room at t=280s

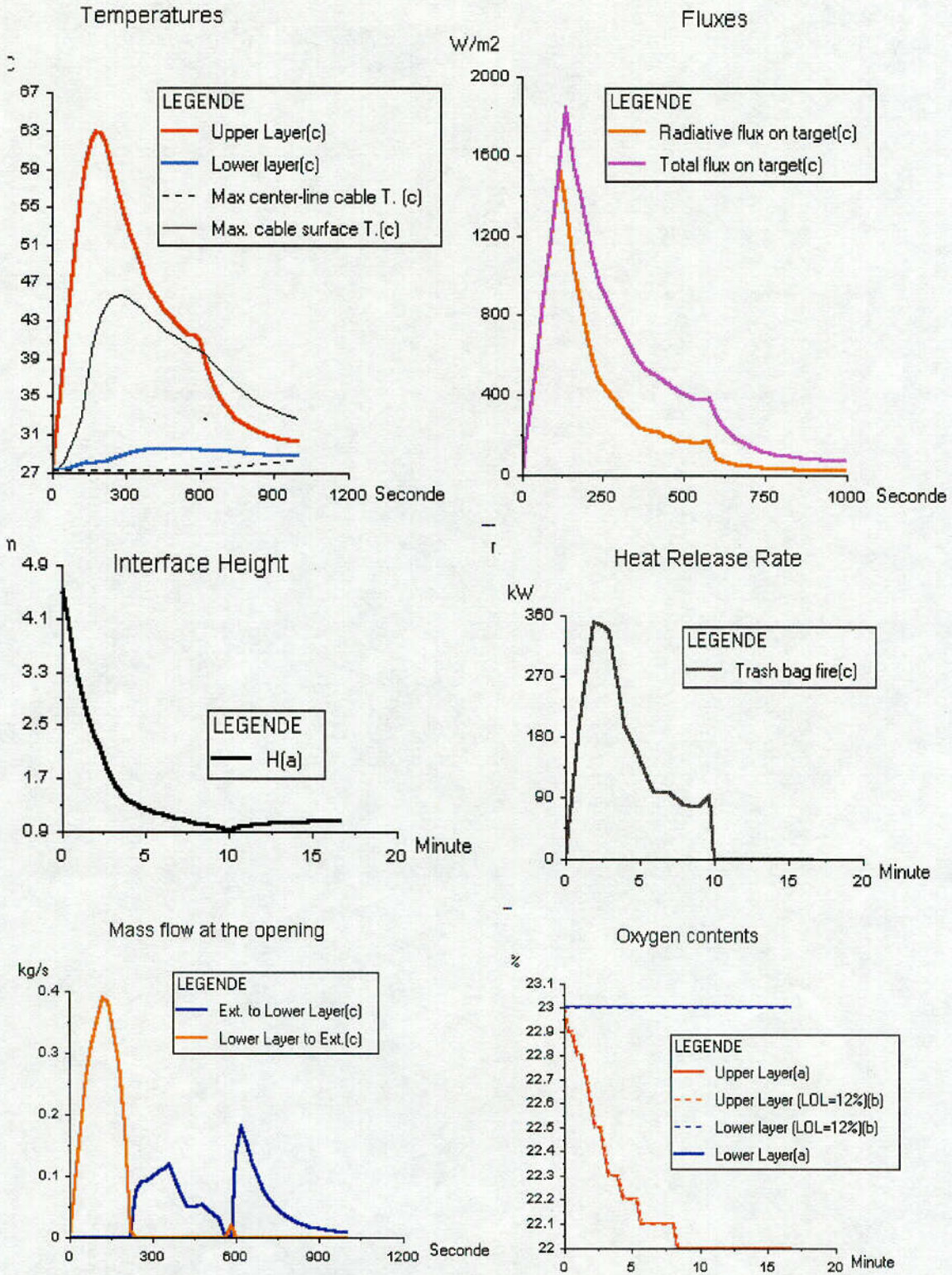


figure 2: part 1 base case

No damage of the target cable is observed in this case . the smoke filling is stabilized (~1m) but temperatures are low. There is not enough consumption of oxygen to show a difference between 0% and 12 % LOL.

C04
196

Effect of ventilation (case 4 and 5)

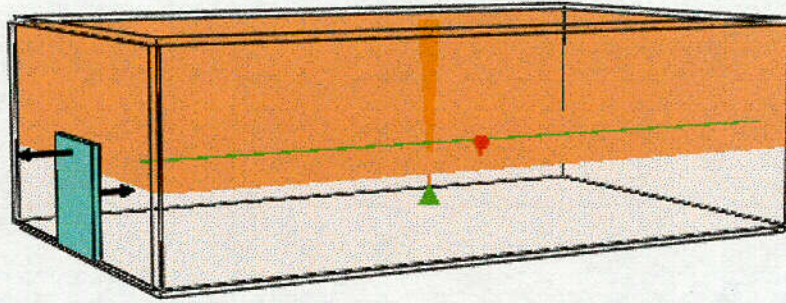


figure 3 : smoke filling in case 4 (door open) at $t=800s$

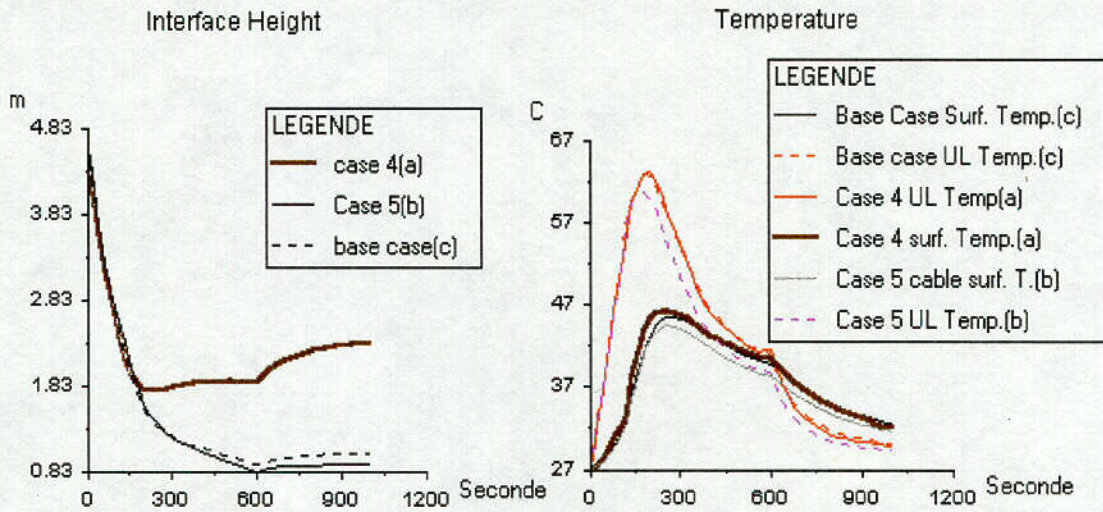


figure 4: ventilation case 4 (door open) and 5 (mechanical vent)

The mass flow balance smoke filling are changed in those two cases: nevertheless, this has no strong effect on the target, which remains in the Upper Layer.

Effect of distance (case 1, 2, 3)

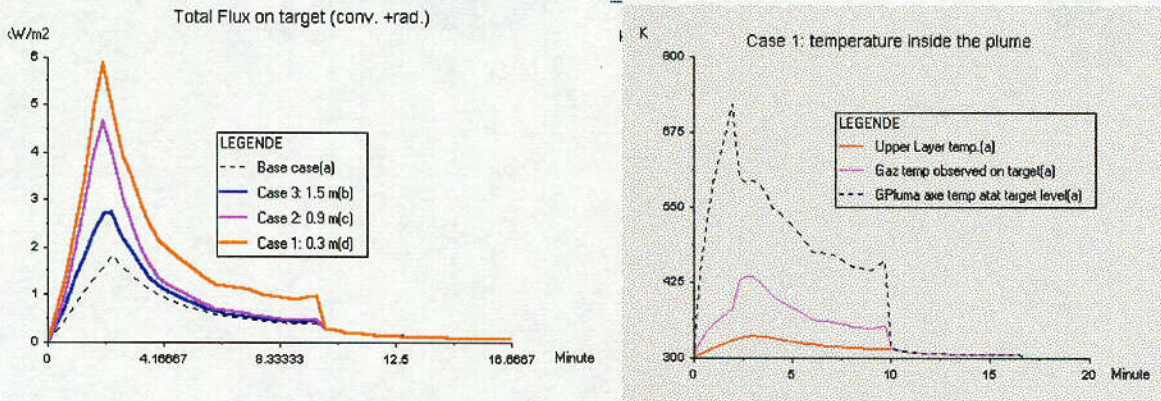


figure 5 : effect of distance

Distance has a strong effect on the radiative flux. The temperature on the target inside the plume is obtained¹ through the Heskestad correlation, taking into account the distance to the axis. As the temperature given by this correlation decreases quickly with the distance to the axis, it can be more conservative to consider the target on the axis (figure 5).

Part II : result analysis

Base case

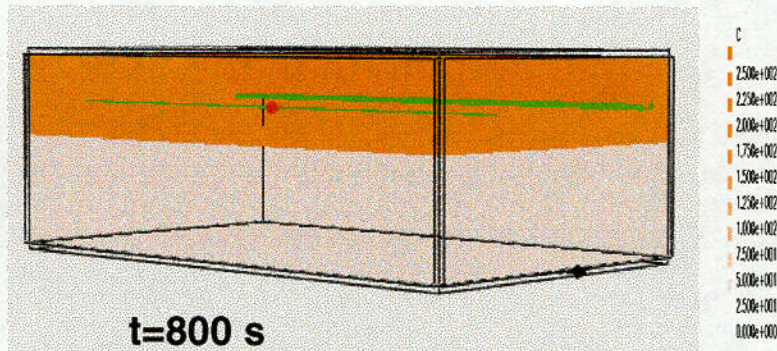


figure 6: smoke filling in part II base case at $t=800$ s

In the base case of part II, no damage of the redundant cable in tray B was obtained. In fact this is due to the lack of oxygen: even if the source is more important, the heat release becomes quickly weak. Note than in this case, the standard MAGIC thermal model of cable was used.

¹ Unlike what was said during the slide presentation...

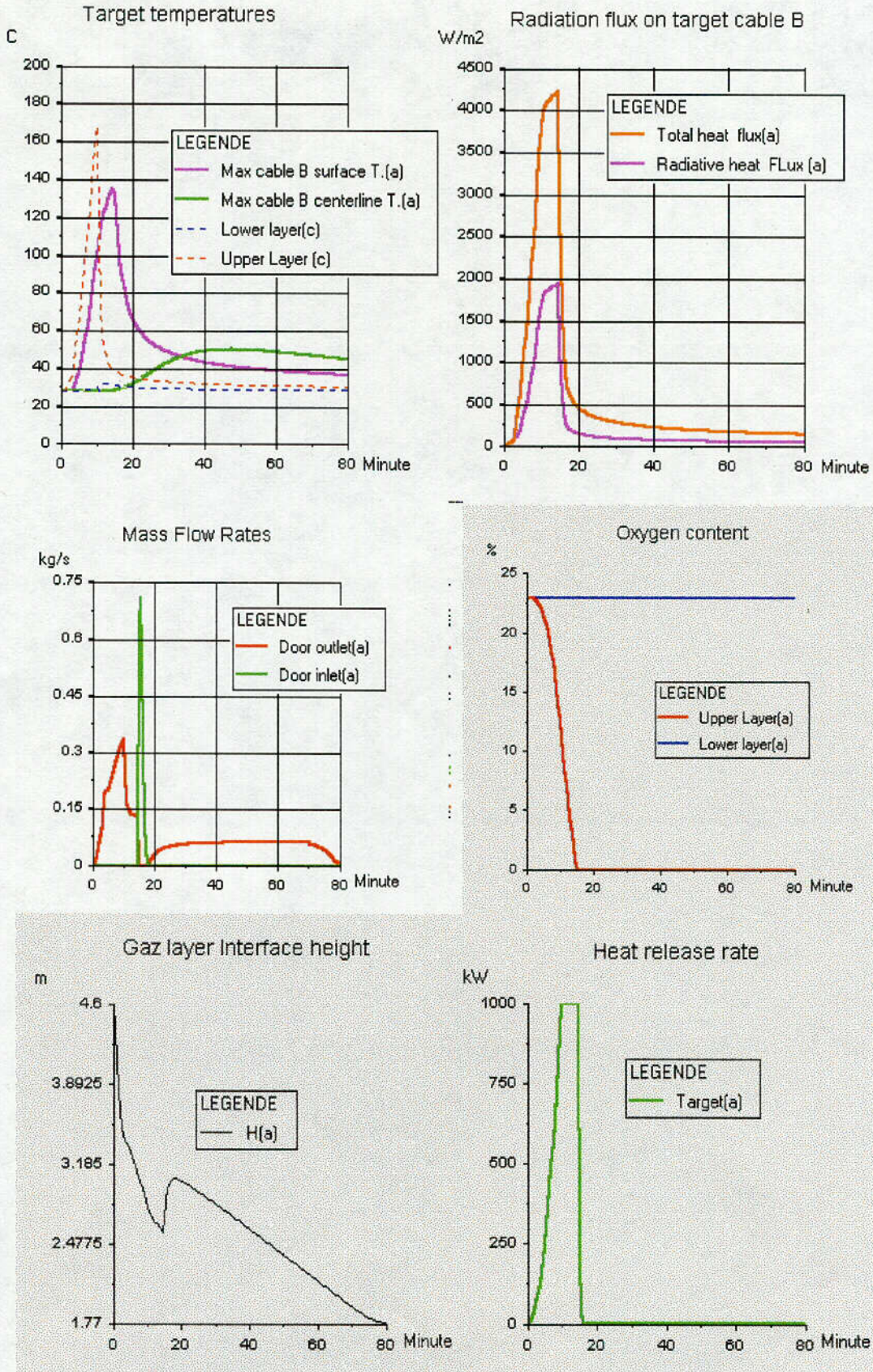


Figure 7: Part II Base case (LOL=0%)

C07
149

Effect of the LOL

Unlike in part I, the results obtained in part II with a LOL of 12% or a LOL of 0% are quite different. Here, we have an oxygen limited fire, has shown in figure 8. The heat release can be performed further in case LOL=0%, with significant influence on the target temperature peak.

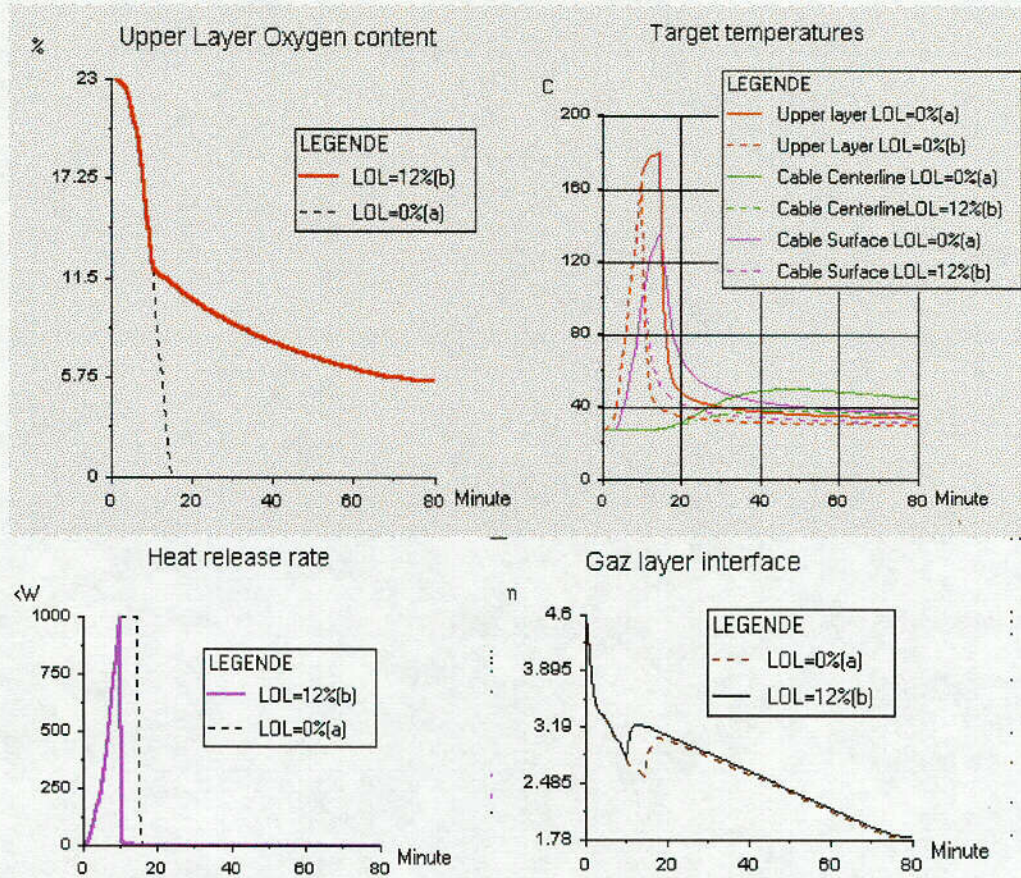


figure 8: effect of the LOL

Mass loss rate increase (case 3-8)

Due to the existing lack of oxygen, the increase of mass loss rate has no significant effect on the fire, which is controlled by the ventilation rate. This is even more true with $LOL=12\%$.

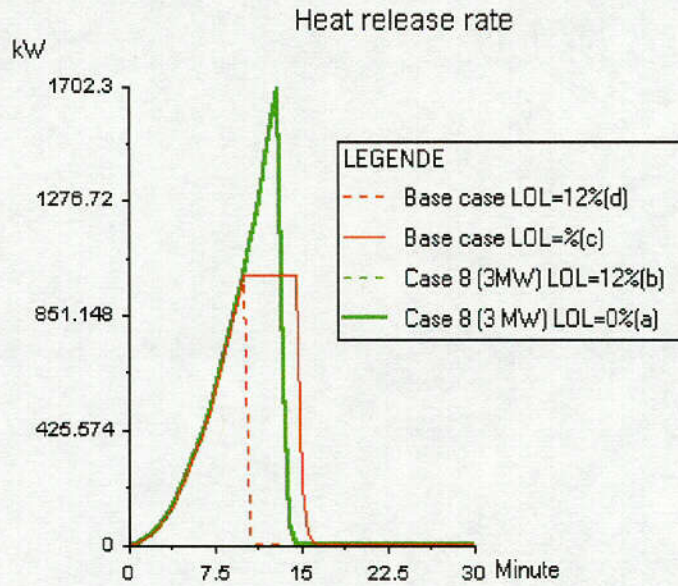


figure 9: mass loss increase

Ventilation effects (cases 9-10)

Due to oxygen rate depletion below the ceiling, the fire conditions are not noticeably changed.

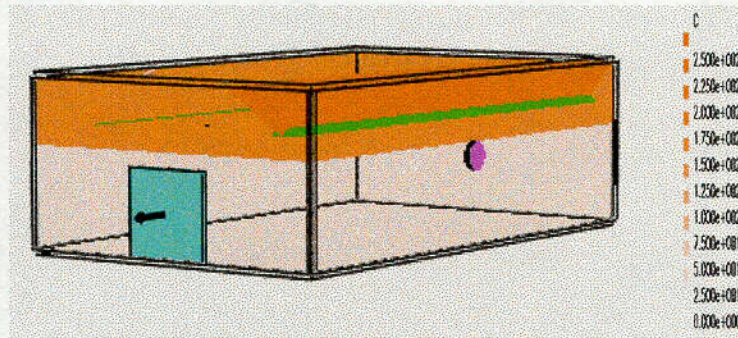


figure 10 : smoke filling at $t=600s$ in case 9

C09
151

Effect of the cable structure and elevation (cases 13 and 11)

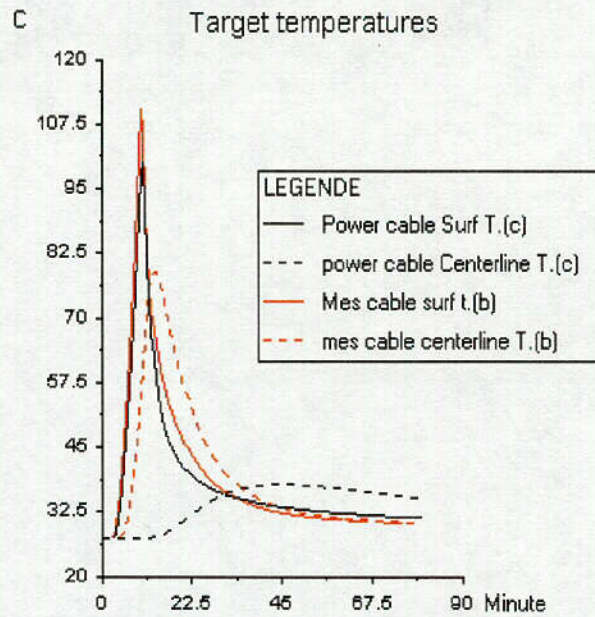


figure 11: effect of cable structure and elevation

The structure of the cable has a strong effect on its resistance: the power cable has more inertia and resists longer (figure 11).

In case 11, the influence of the target elevation is not significant: cable B remains outside of the ceiling-jet region. In fact this point should be discussed further, for the ceiling-jet model is not calculated for $R/H > 3$, this value being the limit of the validation field (COOPER model [1]). In any case, the target model is not connected to the ceiling-jet model in Version 3.4.7 of MAGIC. In the present case, the cable should be considered lost in a real life risk study.

Result summary

Part I :

Part I	O2 Conc. @ 600s (%)	Max Plume Flow (kg/s)	Max Pressure (Pa)	Max outflow (kg/s)	Layer Ht @ 240s (m)	Max UL Temp (K)	Max flux on Target (W/m2)	Max. Target CL Temp (K)
Base Case	R: ZC 22%	NA	R: 961 Pa	R-from LL: 0,389kg/s	R: 1,37m	R: 336 K	Rad: 1550,6 W/m2 Total: 1839 W/m2	R: 301,3 K
Case 1							Rad: 11648,8 W/m2 Total: 12855 W/m2	R: 302,9 K
Case 2							Rad: 4654 W/m2 Total: 4665 W/m2	R: 302,3 K
Case 3							R: 2688 W/m2 Total: 2732 W/m2	R: 301,6K
Case 4			R- for neg peak: 0,1Pa	R- form UL 0,855kg/s	R: 1,77m	R: 336 K	R: 1545 W/m2 Total: 1845 W/m2	R: 301,4 K
Case 5	R: ZC 22,5%		R: 714 Pa		R: 1,43m	R: 333,6 K	R: 1571 W/m2 Total: 2042 W/m2	R: 301,3 K

Part II:

Part II	O2 Conc. (%)	Max Pressure (Pa)	Time @ (s)	Max UL Temp (K)	Max flux on Target (W/m2)	Max. Target CL Temp (K)
Base Case	R- @ 500s: 17%	R-for pos peak: 721Pa	Layer Ht=3,4m: 206s	R1: 452,5 K R2: 440 K	R1: rad 1920W/m2 Total: 4207 W/m2 R2: rad 1677W/m2 Total: 3785 W/m2	R1: 322,6 K R2: 310,7 K
Case 1					R1: 1920W/m2 Total: 4208 W/m2 R2: 1677W/m2 Total: 3785 W/m2	R1: 322,5 K R2: 310,7 K
Case 2					R1: 1920W/m2 Total: 4208 W/m2 R2: 1678W/m2 Total: 3784 W/m2	R1: 322,5 K R2: 310,7 K
Case 5					R1: 3165 W/m2 Total: 6205 W/m2 R2: 1678W/m2 Total: 3785 W/m2	R1: 322,2K R2: 310,7K
Case 10	R- @ 3800s R1 0% R2 5,77%		Layer Ht=2,4m no value	R1: 453,5 K R2: 440,8 K	R1: 1938,2W/m2 Total: 4238 W/m2 R2: 1681W/m2 Total: 3792 W/m2	R1: 322,2 K R2: 310,7 K
Case 11					R1: 1920W/m2 Total: 4207 W/m2 R2: 1677W/m2 Total: 3784 W/m2	R1: 322,6 K R2: 310,8 K
Case 12					R1: 1000,8W/m2 Total: 1119,8 W/m2 R2: 832,5W/m2 Total: 877 W/m2	R1: 306 K R2: 302,6 K
Case 13						R1: 398,1 K R2: 351,7 K

Plume flow is not a standard output of MAGIC. All results are in acceptable domain.

Discussions

About uncertainties...

Like the physical models choices are fixed in MAGIC, the calculation uncertainty can be related to the limits and the accuracy observed in the field of validation of the model, and to the user input uncertainties. It is difficult to define a exhaustive rule for the validation field. In the validation file, the experimental configurations present compartments from 10 to 1300m³, fire source from 100 kW to 2,5 MW. The results obtained are globally satisfactory, with different accuracy in each test.

The most significant input parameter are the source power, the thermophysical parameters (k, h, C, ρ) and source characteristics (stoichiometry , radiative part, etc..).

...and user effect

The "User Effect" is limited as much as possible through the graphical (3D) control and the tests performed by the interface (definition range of values, coherency of the building). The stronger user effect has been observed on conduction meshing : significant errors can be committed on gas temperature in the dynamic steps when the meshing is not fine enough. That the reason why this input will be automated in the next version of the code.

The second user parameter identified was the wall effect on the plume . In this case no significant effect (less than 1 °C) can be observed on temperatures.

The interpretation of result data is a strong source of user effects: for instance in MAGIC the cable behavior is not accurately evaluated inside the plume or ceiling-jet. In EDF practice, we consider than a cable is lost when in a plume of Ceiling-Jet. This is an example of the good knowledge of the code feature needed.

Another example is the cable dysfunction criterion. It can vary from one author to another and is very important in safety assessment. This is an example of the good methodology needed.

Models used in MAGIC and significant for the tests

A short summary of the models used in Magic would be:

- the plume and flame experimental entrainment correlation from MAC CAFFREY^a
- an integrated radial conduction model for cables
- a 1D conduction model into walls, ceiling and floor
- a semi-transparent radiation model for gas, and a radiosity system for walls,
- HESKESTADT correlation for flame height^b and thermal targets.
- a medium specific area model for opacity of cable smokes^c (BARAKAT-VANTELON)
- a Ceiling-Jet^d (L.Y. COOPER)
- "Bernoulli" flow at vertical vent (CURTAT-BODART)

The physical models resulting from the integration of physic laws have no other domain limits than those of the material properties. For (a) (b) (c) and (d) , specific domain limits have been defined in the original experimental works.



Validation of MAGIC

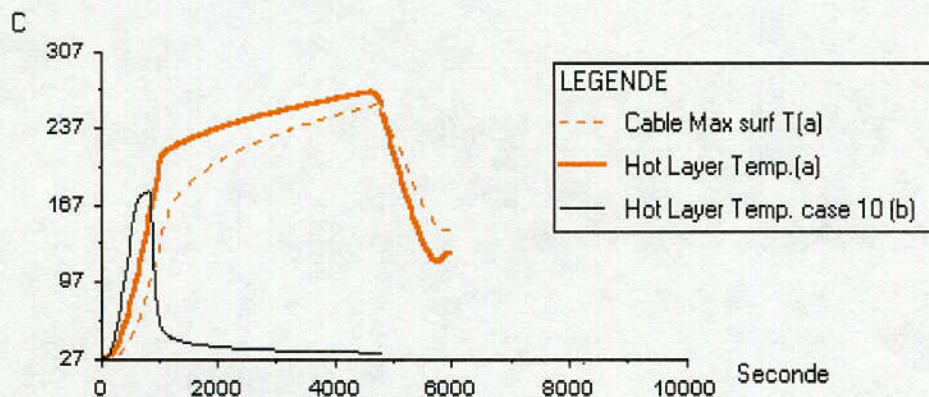
The type of configuration (power, room-size) proposed in the benchmark is well represented in the Validation File of MAGIC [2]. This validation concerns mainly field temperatures and fluxes. The cable center temperature model has been validated at laboratory scale in a "Tewarson" calorimeter device through an EDF experimental program [3].

The validation process of MAGIC gives an idea of the calculation uncertainties. In general, conservative errors are less regarded than "unconservative" ones, for design purpose. For instance, calculated temperature are rarely less than 10°C lower than measurement, but 50°C higher than measurement can be observed.

The flux calculation is less accurate due to many experimental effects. A 50% lower than measurement can be observed. Mass flows are often not available (significant measurement uncertainties).

Effect of the source height

Source height is an important parameter that could have been considered in the benchmark, especially when a door is open (cable trays can be found in lower location). A supplementary calculation has been done in that way (figure 12).



Part II: Effetc of a lower location of cable fire : 1 m above floor in case 10

figure 12: effect of a lower fire source location

The comparison with case 10 shows that the consequences of the fire are quite different: due to the oxygen feeding by the open door, the fire can go on. In this case, cable B would have been probably lost.

Conclusion

The conclusion will follow the suggested guide line [5].

Capability and strength of code MAGIC

From the physical modeling point of view, capability and strength of code MAGIC could be summed up in:

- the global energetic balance done and the good prediction of the level of temperature within the room
- the targets and cable flux and thermal behavior models
- the mass flow prediction by taking into account pressure,
- the calculation of oxygen balance and consumption
- the good level of the radiation model and the wall conduction model
- the good level of information and control provided by the interface (see further).

Weaknesses and limitation:

The behavior of cables is not modeled into plume and flame (cables are considered lost in EDF approach in those cases). This point could be enhanced. The thermal target give a "correlated" response in those cases (Heskestadt model).

The zone model can't represent some 3D aspects like aerualic "by-pass". A conservative approach is used considering that all the oxygen given to the plume can be used. Some real scale fire tests have shown that confined fires could be maintained with a measured O₂ concentration lower than 10%. In those cases, aerualic by pass and distant flame were observed. For this reason, EDF does not use the Low Oxygen Limit in safety studies.

The most important criticism one can make about the MAGIC fire model is that mass loss and thermal behavior of source are not coupled. It is the same for most of the existing codes, apart some very specific cases. The problem is that this coupling is really a difficult problem, especially for solid fire. This can be balanced by using characteristic mass loss profile for one given combustible in one given situation. This type of profile is at the center of the methodological discussions for safety assessment.

Need of a more advanced model?

Maybe the most significant progress has to be made on the mass loss rate of the cable. On this aspect a lot of studies have been done [3]. It seems that a complete fire spread model coupling heat release and mass loss could only be proposed in CFD codes, due to the level of local information needed. For common purpose, one will have to use standard profiles and correlation. An important discussion on this data should be held in the nuclear assessment field to agree of the more adapted ones.

Another important point is the target behavior which could be enhanced in the "dynamic" zones (plume, ceiling-jet). Adapted real scale tests would be of interest, especially for thermal behavior of cables.

Could a simpler model be sufficient in those cases?

In some cases a simpler model can be adapted, but cable thermal response, oxygen consumption balance and ventilation effects had to be taken into account in the cases studied here. That means a minimum of balanced model is necessary: zone models are the minimum level of modeling needed here.

Additional type of model needed:

Cable behavior inside the plume or Ceiling-jet would be of interest. Of course, more information would necessary here.

User Interface of MAGIC

The user interface is probably one of the most outstanding strengths of code MAGIC. Many automated controls are performed on value definition range, building coherency, and the graphical 3D view provide a powerful visual control to the user. The use of such an integrated interface limits notably the risk of input mistake.

Nevertheless, the user must be aware of some aspects of zone modeling not to forget:

- the conservative approach of phenomena (ex: combustion efficiency)
- the rough representation of air stratification temperature
- some 3D aerualic and flame effects are not considered (ex: horizontal distance ventilation/source) but over-predicted (always conservative).

Outlook

The most relevant parameter in the deterministic fire modeling is certainly combustible mass rate. There is a great need here for conventional curve profiles or formulas, and experimental process for cable behavior identification. We should define a consensus mass loss profile data file

On that point, from EDF experience we should at least consider:

- not confined cable tray with low ignition (slow spread)
- not confined cable tray with strong ignition (up to ~x00kW: fast spread)
- confined cable trays (in smoke) : "flashover" (global instantaneous ignition)

Cable or component dysfunction is another important parameter

- the cable temperature criterion has to be enhance. Internal temperature of cable seems to be a reliable variable to correlate [7].
- on that point, experimental test benches could be normalized

Multi-room configuration is also an essential issue. For instance, in EDF NPP configuration, component in the first room are always protected if concerned by safety issues : what is important and has to be modeled is what happen to component in secondary rooms. For this reason, it would be of interest to propose more multi-room configurations in the future benchmarks...

To conclude, we should remind the "good way" to process is to go from the more conservative to the more complex: in safety assessment, one should use simple (conservative) formulas or models when sufficient and go into details with zone or CFD codes when necessary. If the methodology is

organized in that way, it will be easier to promote the use of numerical model in the fire risk assessment.

REFERENCES

- [1] B. GAUTIER, O. PAGES "MAGIC software version 3.4.1: mathematical model" EDF HT-31/99/007/A.
- [2] B. GAUTIER, Ch. LE-MAITRE "Validation file of Software Magic Version 3.4.1". HT-31/99/002/A Feb.99.
- [3] E. THIBERT "*Modélisation de la combustion des gaines de câbles électriques*" Thesis from University of Poitier-FRANCE Nov. 1999.
- [4] M. Dey "International Collaborative Project to Evaluate Fire Models for Nuclear Power Plant Applications, Benchmark Exercise # 1: Cable Tray Fires of Redundant Safety Trains: definition of scenarios" NRC September 11th 2000.
- [5] M. Dey "suggested guideline/questions for presentation of Results of Benchmark Exercise".NRC 2000

**Appendix D: Benchmark Analysis with CFX, Matthias
HEITSCH, GRS, Germany**





Gesellschaft für Anlagen-
und Reaktorsicherheit
(GRS) mbH

CFX Simulations for the Benchmark Exercise #1 - Cable Tray Fires of Redundant Safety Trains -

International Collaborative Project to Evaluate Fire Models
for Nuclear Power Plant Applications

Dr. Matthias Heitsch

Technical Note HET 1/2001

Gesellschaft für Anlagen- und Reaktorsicherheit (GRS) mbH
Schwertnergasse 1
D-50667 Koeln
Tel: +49 221 2068 678
Fax: +49 221 2068 834
Email: het@grs.de

Content

	List of Figures and Tables	4
	Abbreviations	6
1	Introduction.....	7
2	The CFD Code CFX.....	7
3	Analyses on Part 1.....	8
3.1	Base Case	9
3.2	Case 1.....	10
3.3	Case 5.....	10
4	Analyses on Part 2.....	11
4.1	Base Case	12
4.2	Case 6.....	12
4.3	Case 10.....	13
5	Summary.....	13
6	Continuation of Work	14
	References.....	14
	Figures and Tables	15



List of Figures and Tables

Fig. 1	View of the room to be modeled.....	15
Fig. 2	View of the computer model for part 1.....	16
Fig. 3	Overview of given heat release over time (Part 1)	16
Fig. 4	Temperature distribution at the time of strongest heat release (base case)	17
Fig. 5	Lateral view of the fire room after 180 s (base case)	18
Fig. 6	Temperature distribution after 600 s (base case).....	19
Fig. 7	Vertical temperature profile from bottom to top after 600 s (base case) ...	20
Fig. 8	Heat absorbed by the target cable (base case).....	21
Fig. 9	Target cable surface temperature variation for the base case	22
Fig. 10	Flow field and temperature distribution in the room for case 1	23
Fig. 11	Heat fluxes for case 1	24
Fig. 12	Surface temperature over time for case 1	25
Fig. 13	Flow field in the fire room with ventilation system on (case 5)	26
Fig. 14	Cable surface temperature with case 5	27
Fig. 15	Comparison of surface temperatures for benchmark part 1	28
Fig. 16	CFX model for benchmark part 2.....	28
Fig. 17	Temperature distribution after 1200 s (base case).....	29
Fig. 18	Given heat release rate over time (part 2, base case)	30
Fig. 19	Heat absorbed by the target cable (part 2, base case)	31
Fig. 20	Target cable temperatures during the base case of part 2.....	32
Fig. 21	Temperature distribution after 700 s for case 6.....	33
Fig. 22	Target cable temperatures for case 6.....	34
Fig. 23	Profile in the center of the room for base case and case 6	35
Fig. 24	Heat flows to walls and target cable for case 6	36
Fig. 25	Temperature stratification after 4200 s for case 10	37
Fig. 26	Side view of the room at the end of the maximum power release.....	38
Fig. 27	Target temperatures over time for case 10	39
Fig. 28	Comparison of cable temperatures for base case, case 6 and case 10 ...	40

Tab. 1 Summary of results of simulations.....41

(102)

Abbreviations

CFD	Computational Fluid Dynamics
NPP	Nuclear Power Plant

1164

1 Introduction

A benchmark exercise has been set up to evaluate the capabilities of codes to model relevant phenomena with cable tray fires in a NPP. According to the specification of this Benchmark Exercise part 1 [DEF 00] out of the large number of numerical cases specified a representative selection has been simulated by the help of the general-purpose CFD code CFX 4.3. The motivation of the application of CFX has been to find out how it performs in comparison with other probably more specialised codes. It is also of interest under which conditions the specific characteristics of CFX are beneficial and can justify the higher computing costs. So far, due to restrictions in the computing resources available not the complete suite of specified test cases has been simulated. However, the presented selection is believed to provide a good idea of the capabilities when applying CFX. Work will be continued based on the experience got from the meeting in Palo Alto in January 2001.

2 The CFD Code CFX

The code CFX-4.3 [AEA 99] provides numerical approximations of the Navier-Stokes equations on a finite volume basis. The program version applied here uses a block-structured grid with body fitted coordinates. Block-structured means that all blocks of the computational domain have to be designed with a hexahedral shape. With complex geometries this implies occasionally finer grids than really necessary.

The code offers a number of physical models to simulate a wide range of flow problems. Among these are:

- Arbitrary multi-component mixtures,
- Turbulence models for low and high Reynolds numbers,
- Multi-phase models including a versatile multi-fluid model and a homogeneous two-phase model,
- Particle transport model,
- Complex thermal radiation model based on a Monte-Carlo formulation,

- Chemical reaction capability,
- Convective heat transfer and heat conduction,
- User Interface to modify existing or add own models.

The given benchmark makes use of the turbulence (k- ϵ) and multi-component models combined with the thermal radiation package. Chemical reactions, although possible, are not included in the simulations so far.

3 Analyses on Part 1

In part 1 of the benchmark exercise a trash bag fire in the vicinity of a cable tray inside an emergency switchgear room (Fig. 1) is to be simulated. The objective "is to determine the maximum horizontal distance between a specified transient fire from the trash bag and tray A (Fig. 1) that results in ignition of tray A" [DEF 00]. For simplicity the cable tray represented by a single power cable of 50 mm. The room has ventilation and a fire proof door. A base case and five related simulations with variations of the distance between cable tray and fire, the door open or closed and the ventilation system on or off are to be investigated. The time to be covered is 600 s. The total heat release from the trash bag is specified in Fig. 3 and the radiative fraction is fixed to be 30%. This specification implies not to simulate the chemical reactions in the trash bag explicitly rather than using the heat release curve and study the convective and radiative flows induced by the fire in the trash bag.

A computer model was developed which is composed of 28400 fluid cells (Fig. 2). The grid resolution could be refined easily but is left on this rather crude level to comply with the number of test cases and the problem time of this exercise. The model contains the trash bag and the target cable (representing tray A) inside the room. In order to save computing time the outer walls are not modeled. This results in an overestimation of the heat losses from the fire room atmosphere because the heat up of inner wall sections is neglected and consequently the temperature difference gas to wall is too large. The given convective heat transfer coefficient of 15 W/m²K is applied. For some of the cases the openings of the ventilation system and the fire door can be opened. In all other cases a crack of specified size around the door is available.

156

There are several options to implement the heat release from the trash bag. Currently the trash bag is modeled as a solid body with the convective fire heat release from the nearest cells around it and with radiation from its surface. The trash bag could also be a hollow body with the convective heat released from all the internal cells. Because radiation can only be emitted from a surface, in this case the top surface could be used for the radiation source. The benchmark specification does not further localize the heat sources therefore the first option has been implemented. During the simulations it turned out that the shape of the trash bag fire changed from time to time. However if numerical reasons or inherent instabilities cause this behavior has not been further investigated.

Conduction in the target cable is included. The cable itself is represented as a cylinder of appropriate size and can be moved within the grid according to the different test cases.

The atmosphere within the fire room is assumed to be air. Individual gas species are not modeled because the fire chemistry is not included.

3.1 Base Case

In the base case the target cable has a horizontal distance of 2.2 m from the trash bag. The door is closed and the ventilation system is off. It is the first case simulated and is discussed in more detail. The moment of the highest heat release from the trash bag is depicted in Fig. 4. The plume around the trash bag and the induced upwards directed flow is influenced by the option of the heat release chosen and may be different if modeled by the other option (see chapter 3). The target cable is affected by a flow directed downwards as indicated in Fig. 4. At the moment of strongest heat release the warmer gas is concentrated below the ceiling of the room as shown in Fig. 5. Some flow is directed towards the crack in the fire door. After 600 s the temperature distribution in the room is shown in Fig. 6. At this time gas temperatures do not show a remarkable stratification. Close to the walls temperatures are lower due to the heat losses resulting from the high heat transfer coefficient given. This behavior is illustrated in Fig. 7. From bottom to top the temperature does not vary much. Underneath the ceiling it increases considerably (buoyant flow) before wall cooling is dominating. With a higher gas temperature the heat flux to the wall increases and provokes a higher temperature gradient compared with the bottom region. From the temperature profile in Fig. 7 a subdivision

of the room into a hot layer above a cold layer appears to be inadequate. Of interest is the distribution of heat flows to walls and target cable. All flows reach their maximum at the time with the highest heat release. The total heat flux to the cable in comparison with the flow to the walls (Fig. 8) is less than the surface ratio. This may be due to the lower wall temperatures. In Fig. 8 decreases the radiative fraction to the cable to a very small value when the fire heat release decreases after its maximum. The hotter cable then loses energy to the cooler walls. The heat captured by the cable does not lead to a measurable increase of the centerline temperature. The surface temperature develops as shown in Fig. 9 and has almost no further increase after the maximum heat flow from the trash bag is passed.

3.2 Case 1

Case 1 differs from the base case only by another location of the trash bag relative to the target cable. The trash bag is directly below the target cable. The moment of maximum heat release is depicted in Fig. 10. Compared with the base case the cable is now completely inside the hot gas stream from the fire. This results in a higher heat-up of the cable surface as shown in Fig. 12. The maximum is now about 550 K. In the base case it was only 360 K. After the maximum heat is passed the surface temperature goes down as well. The power to the cable over time shown in Fig. 11 has a maximum of about 700 W. This is considerably more than in the base case with 500 W. Another difference is the radiative behavior. With this case in the late phase the cable radiates energy to the surroundings and is therefore cooled.

The centerline temperature remains almost unchanged during the simulation time. Other cases with larger distances of the trash bag than the actual will not be able to create higher cable temperatures with a chance of ignition (643 K).

3.3 Case 5

Case 5 is interesting because of the flow patterns influenced by the ventilation system now on. The position of the trash bag is identical to the base case. Compared with the base case the cable is now in a more upwards flow. This is depicted in Fig. 13. Equally, the heat-up of the cable is very similar and remains low (Fig. 14). The ventilation system with a continuous inflow of cold air does not alter things considerably.

Chemical reactions including oxygen consumption have not been modelled. However, an oxygen depletion which might be avoided by the fresh air entering through the ventilation opening is not realistic because of the short simulation time.

A comparison of all three simulated cases in terms of the cable surface temperature is depicted in Fig. 15. With the given ignition criterion only the location of the fire directly below the target cable would have a chance to ignite the cable over a longer time or with a higher heat release.

4 Analyses on Part 2

This part of the benchmark is to "determine the damage time of the target cable tray B for several heat release rates of the tray stack (A,C2, C1), and horizontal distance D. The effects of target elevation and ventilation will also be examined." [DEF 00]. The duration of the fully developed fire is fixed to be 3600 s (including transitions 4800 s). To perform a reasonable number of simulations in a short time the computational grid was set to have less cells than for part 1. It is shown in Fig. 16. The model now has 11400 cells. This includes the cells to represent the solids of the cable trays and the target cable (instrumentation cable of 18 or 50 mm diameter). The simulated fire heat from the trays A, C1, C2, which are lumped together, follows the shape shown in Fig. 18. The peak can be between 1 and 3 MW. The target cable is considered to be damaged when the centerline of the cable reaches 200 C.

The release of the heat from the assumed fire is implemented similarly to part 1. The convective fraction is placed as volumetric source into the cells closest to the cable trays. The radiative fraction of 48% is emitted directly from the solid surfaces.

With the longer simulation time the heat absorbed by the boundary walls and the subsequent rise of the surface temperature should not be neglected. Therefore a one dimensional heat conduction simulation has been added. Compared with an explicit inclusion of the walls (this means by conducting cells) the computing time is negligible.

Chemical reactions are not treated in the simulations. Hence no check for oxygen depletion has been done in the code. Only a crude hand approximation has been done. From the specifications it remains unclear how to proceed with the fire heat release if oxygen depletes for a time but then recovers by the ventilation system.

4.1 Base Case

This case is distinguished from other cases by a peak heat release rate of 1 MW and a distance of the power cable (diameter 50 mm) of 6.1 m. The door is closed and the ventilation system is off.

With the higher heat release and all openings closed it is likely that the available oxygen is exhausted soon. An approximation indicates a time of about 1200 s. This time has been selected for the illustration in Fig. 17. A global circulation can be observed and the temperature is rather uniform.

It is speculative how the case would further develop if oxygen depletes because this is not modeled currently. To be conservative the simulation over the full time and the heat release according to Fig. 18 has been performed.

The heat flow to the cable which is at the same elevation like the burning cable trays leads to a rapid heat up of its surface (Fig. 19). Therefore radiation from the cable to the colder boundary walls is positive which means that the cable loses energy. Consequently the heat-up of the cable is reduced. A look to the cable temperatures gives Fig. 20. Although at the surface very soon high values are reached, in the central part of the cable only about 50 K increase is obtained. Therefore no damage with the given criterion can be detected. This is true either after 1200 s when the available oxygen tends to deplete or after 4800 s when following the given heat release curve to full extent.

4.2 Case 6

The base case is only capable of producing a relatively low heat-up of the target. Among the specified cases case 6 assumes the highest peak heat value (3 MW) in combination with the nearest placement of the target cable to the fire source. With higher heat output from the fire oxygen will deplete earlier. According to an approximation this may be after 700 s. After this time the flow field and temperature distribution calculated by CFX is shown in Fig. 21. A large vortex has developed with a horizontal flow along the floor. Fig. 23 compares the temperature in the center of the room of case 6 with the base case. For both cases simulations have been extended beyond the oxygen depletion point up to the end of the specified fire duration. Case 6 leads to a much higher room temperature. However the early oxygen starvation prevents a target

damage. The centerline temperature reaches values above the damage threshold of 423 K only in the late phase of the simulation. This is shown in Fig. 22. A summary of the heat flows received by walls and the target is illustrated in Fig. 24. Right from the beginning the target becomes that hot that it constantly loses energy to the outer walls. However, by gas convection it is heated further.

4.3 Case 10

Both cases analysed up to now suffer from early oxygen starvation although the fire power might be strong enough to damage the target cable. A fresh air flow through the room might change the situation. Case 10 is comparable with the base case but the door is open and the ventilation system is working. Oxygen depletion has therefore been excluded. The incoming air is cold and forms therefore a stable stratification in the room. Fig. 25 and Fig. 26 illustrate this from different perspectives. The flows out of the door and the ventilation system can be seen. A cooling effect to the target cable is not expected. If oxygen around the burning cable trays is sufficiently available can not be answered unless the migration and distribution of the species involved would be modeled in detail. Under the assumption of abundant oxygen to feed the fire, the cable centerline temperature is calculated as shown in Fig. 27. There is only little heating-up in the center of the cable.

5 Summary

Following the benchmark specification a selection of six cases out of a total of 20 for both parts has been simulated by the CFD code CFX. Despite this reduced number of cases they were selected with the intention to preserve the scope of the benchmark and to get representative results.

The analyses carried out demonstrate the capabilities of CFD codes in simulating fire situations. They also outline the higher effort with respect to computing resources. On a DEC-Alpha Unix machine with about 350 Mflops simulations needed approximately 64 h and 153 h for part 1 (28400 cells) and part 2 (11400 cells), respectively.

In order to keep computing times manageable it was decided to use relatively coarse grids for both parts of the benchmark.

None of the cases analysed leads to a damage of the target cable according to the specified damage criterion for part 1 and 2. This is true if depletion of oxygen is included in the simulations. If these are carried out following the heat release curves to full extent then case 6 leads to cable damage.

6 Continuation of Work

An obvious continuation of the current work is the simulation of other important test cases. Among these are for part 2 case 9 with partial activation of the ventilation system and opening of the door in the room. This will enable to investigate whether oxygen depletion will occur later than in previous cases. A realistic chance of cable damage may involve case 13 with a cable diameter of 15 instead of 50 mm.

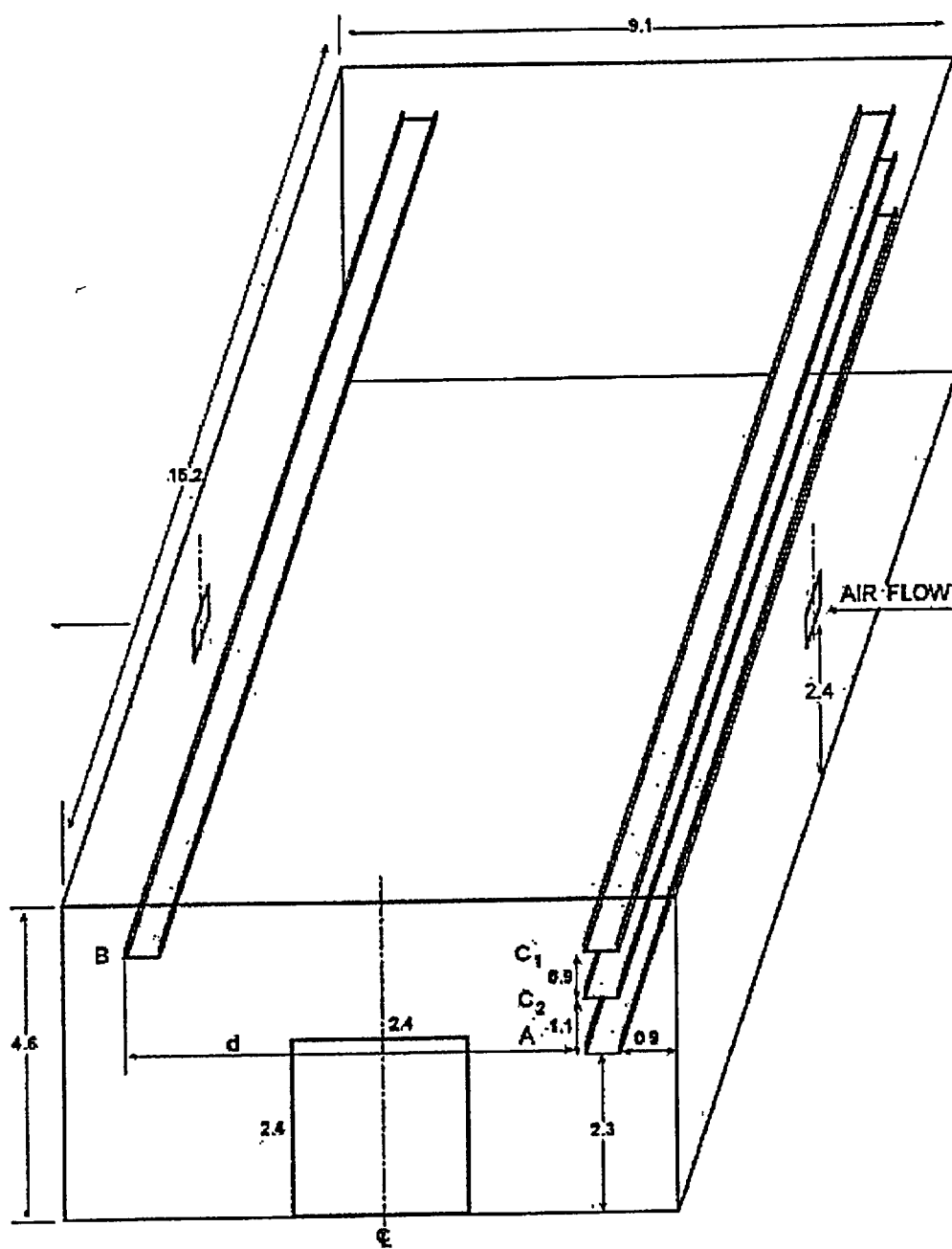
It will be necessary to investigate the quality of the grids for both models applied so far. With finer grid cells at around source and target it can be proved if grid convergence with the solutions found has been achieved.

A crucial point for many cases is the depletion of oxygen. To provide realistic simulations mixing and diffusion of oxygen in combination with the consumption of the fire need to be included into the fire model of CFX. This means that for the relevant species additional conservation equations have to be solved.

References

- AEA 99 CFX4.3, Documentation, CFX International, AEA Technology plc, Oxfordshire, United Kingdom, 1999.
- DEF 00 Benchmark Exercise, Definition of Problem, Revised June 19-20,2000.

Figures and Tables



All dimensions are in meters.

Fig. 1 View of the room to be modeled

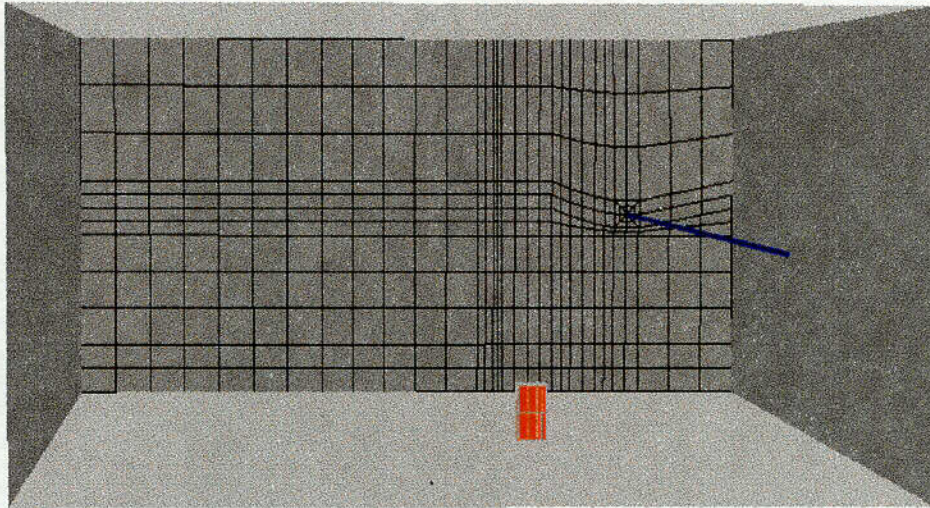


Fig. 2 View of the computer model for part 1

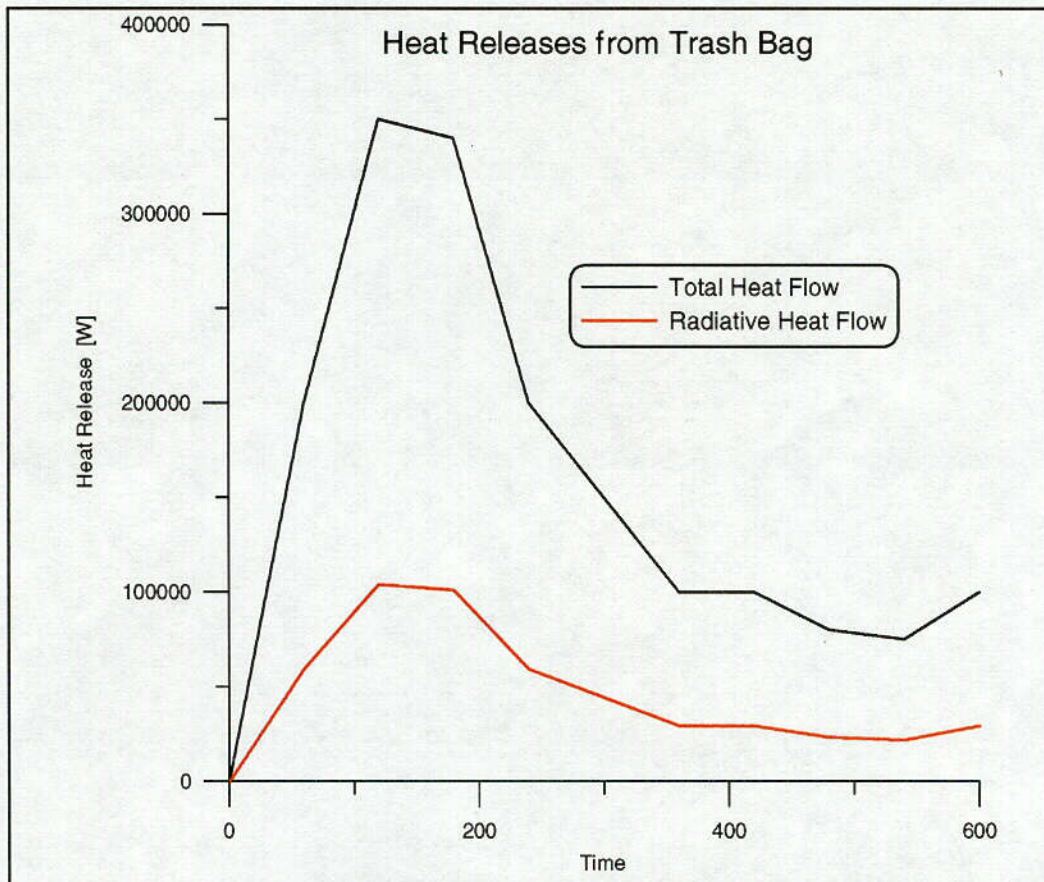
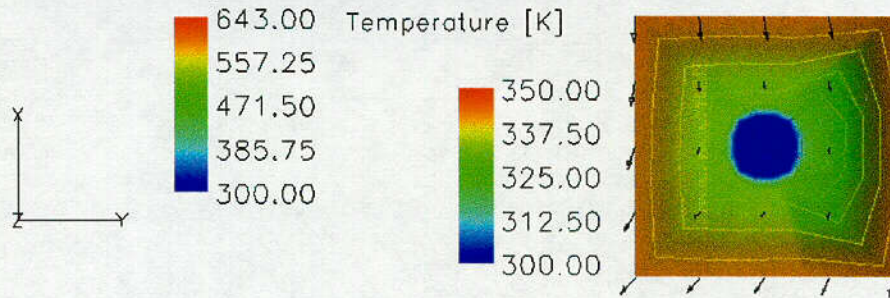
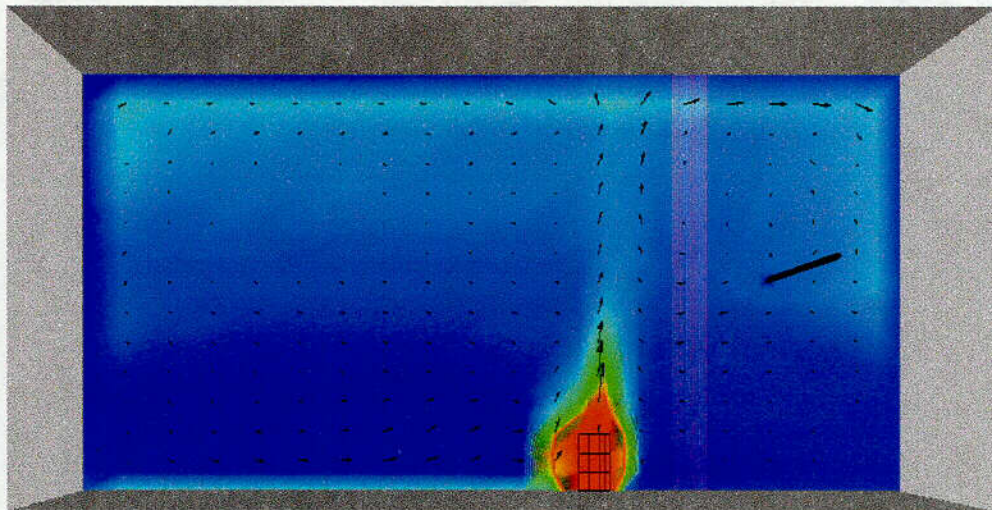


Fig. 3 Overview of given heat release over time (Part 1)

C12
179

Cable Tray Fires of Redundant Safety Trains Benchmark Part I



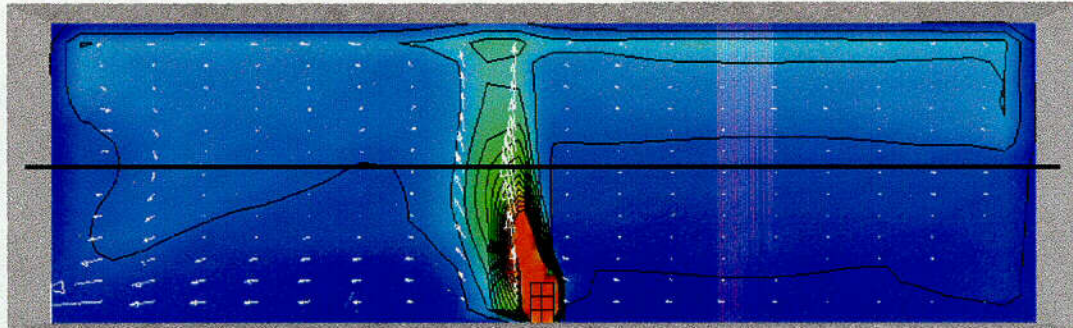
Time=180.35s

Base Case

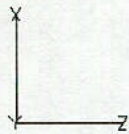
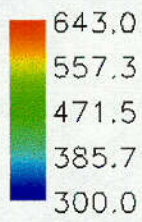
Fig. 4 Temperature distribution at the time of strongest heat release (base case)

C13
175

Cable Tray Fires of Redundant Safety Trains Benchmark Part I



Temperature [K]



Time=180.35s

Base Case

Fig. 5 Lateral view of the fire room after 180 s (base case)

**Cable Tray Fires of Redundant Safety Trains
Benchmark Part I**

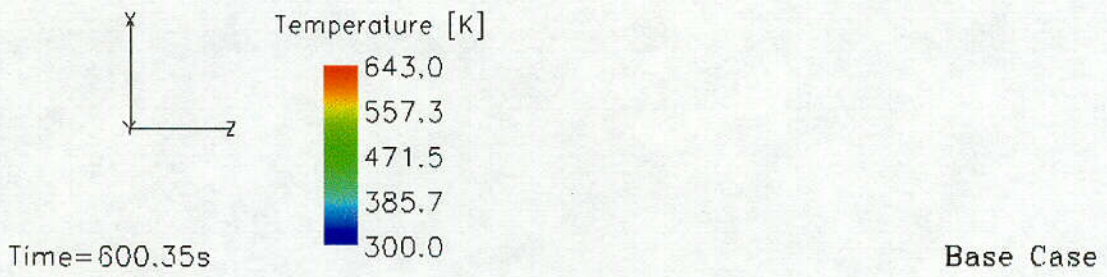
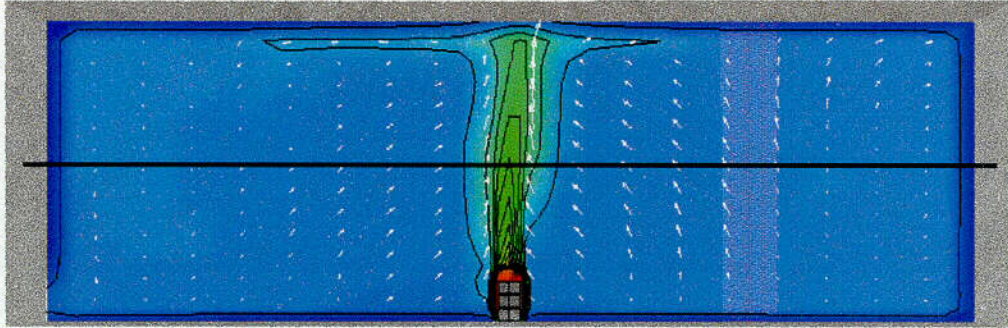


Fig. 6 Temperature distribution after 600 s (base case)

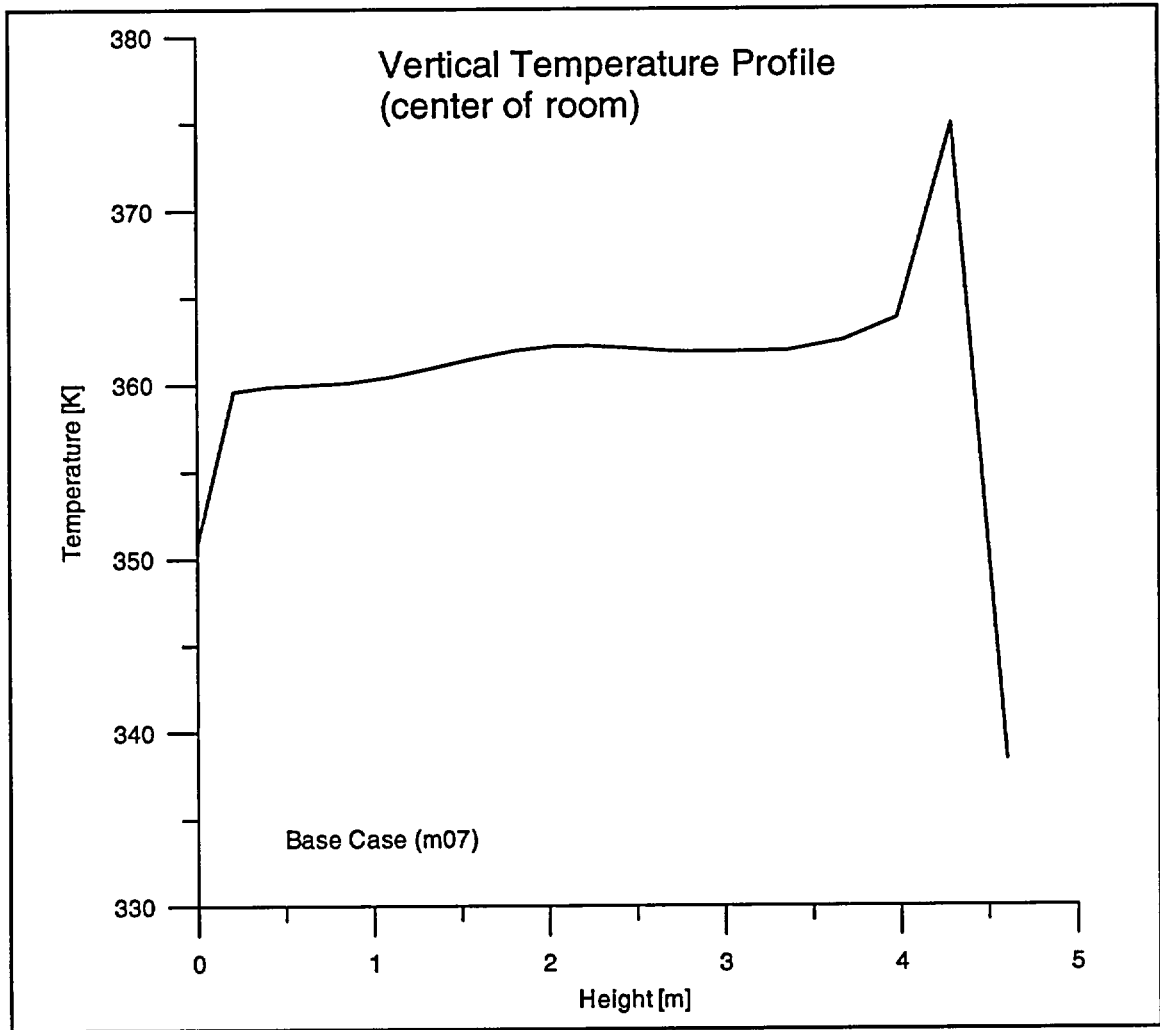


Fig. 7 Vertical temperature profile from bottom to top after 600 s (base case)



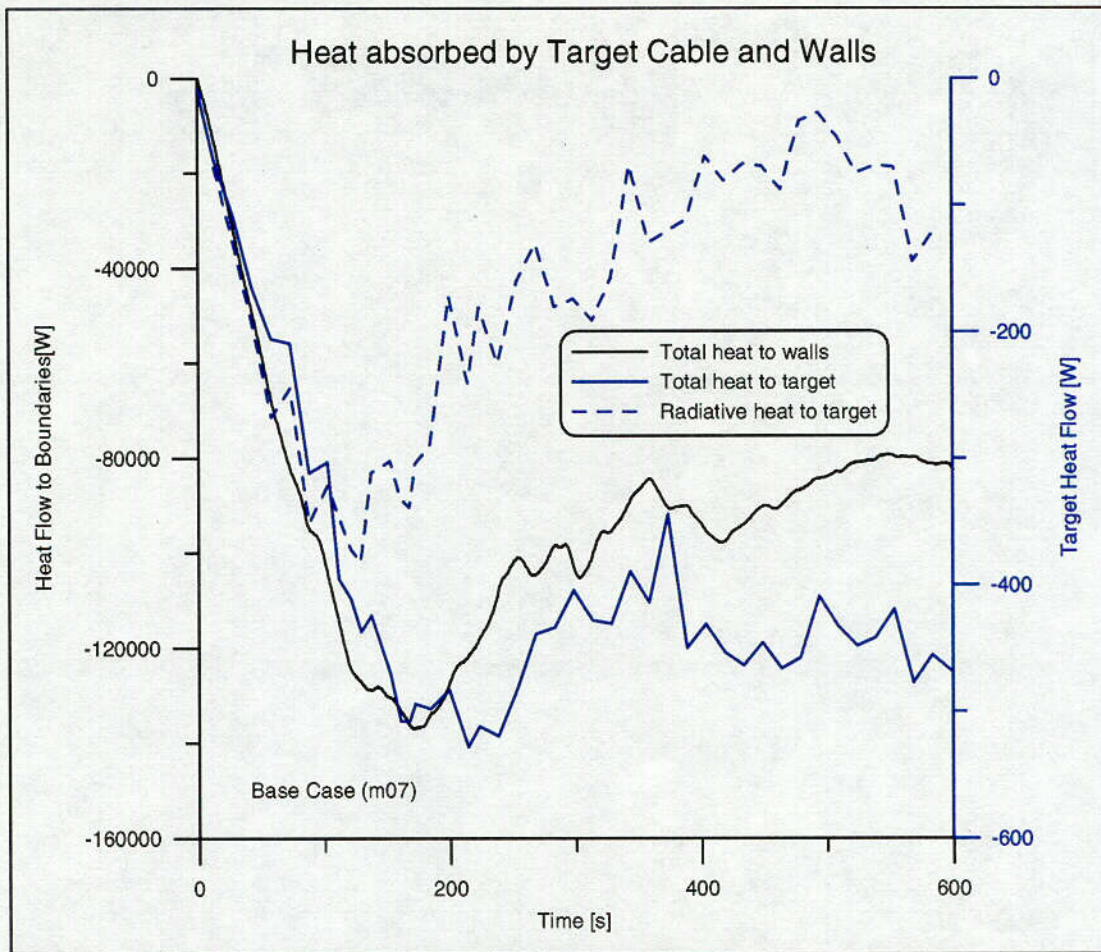


Fig. 8 Heat absorbed by the target cable (base case)

CIG
 179

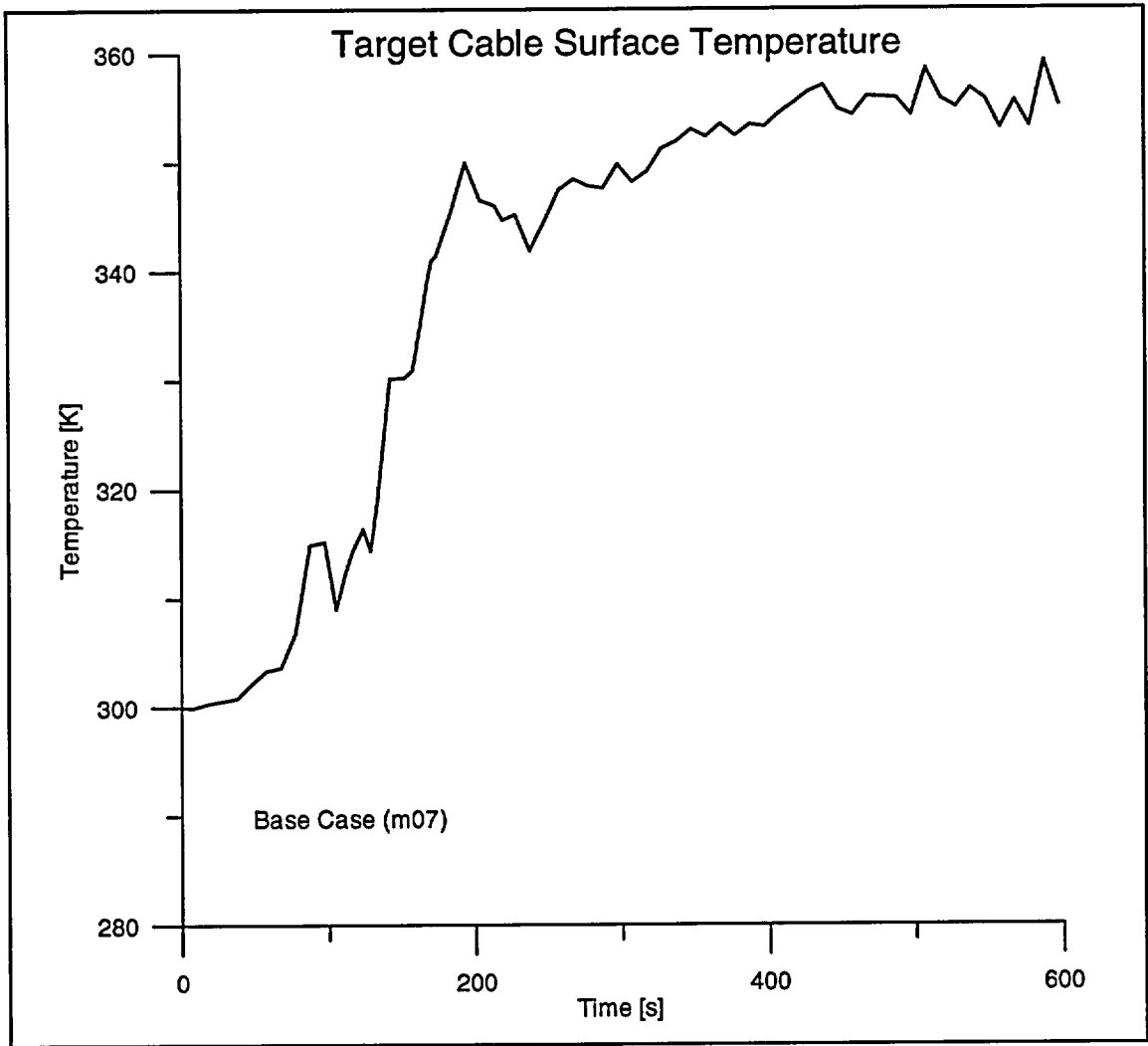
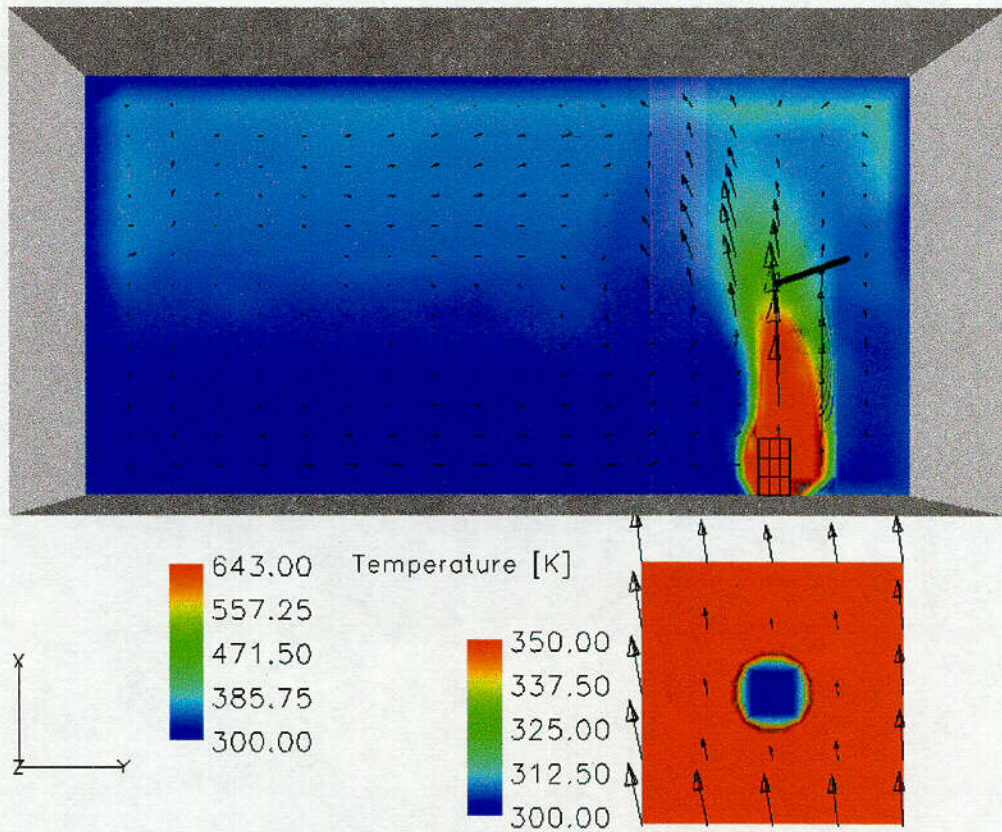


Fig. 9 Target cable surface temperature variation for the base case

180

Cable Tray Fires of Redundant Safety Trains Benchmark Part I



Time=180.1s

Case 1

Fig. 10 Flow field and temperature distribution in the room for case 1

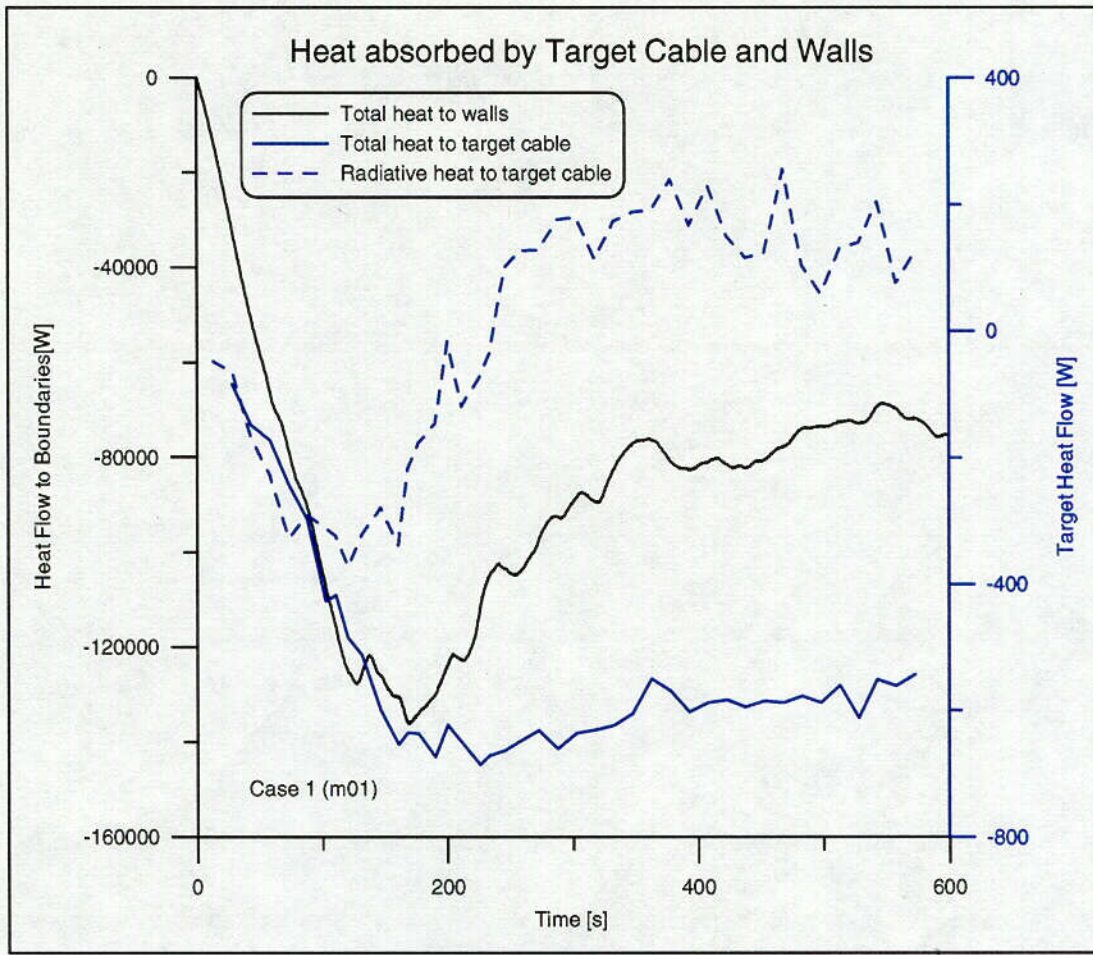


Fig. 11 Heat fluxes for case 1

C19
182

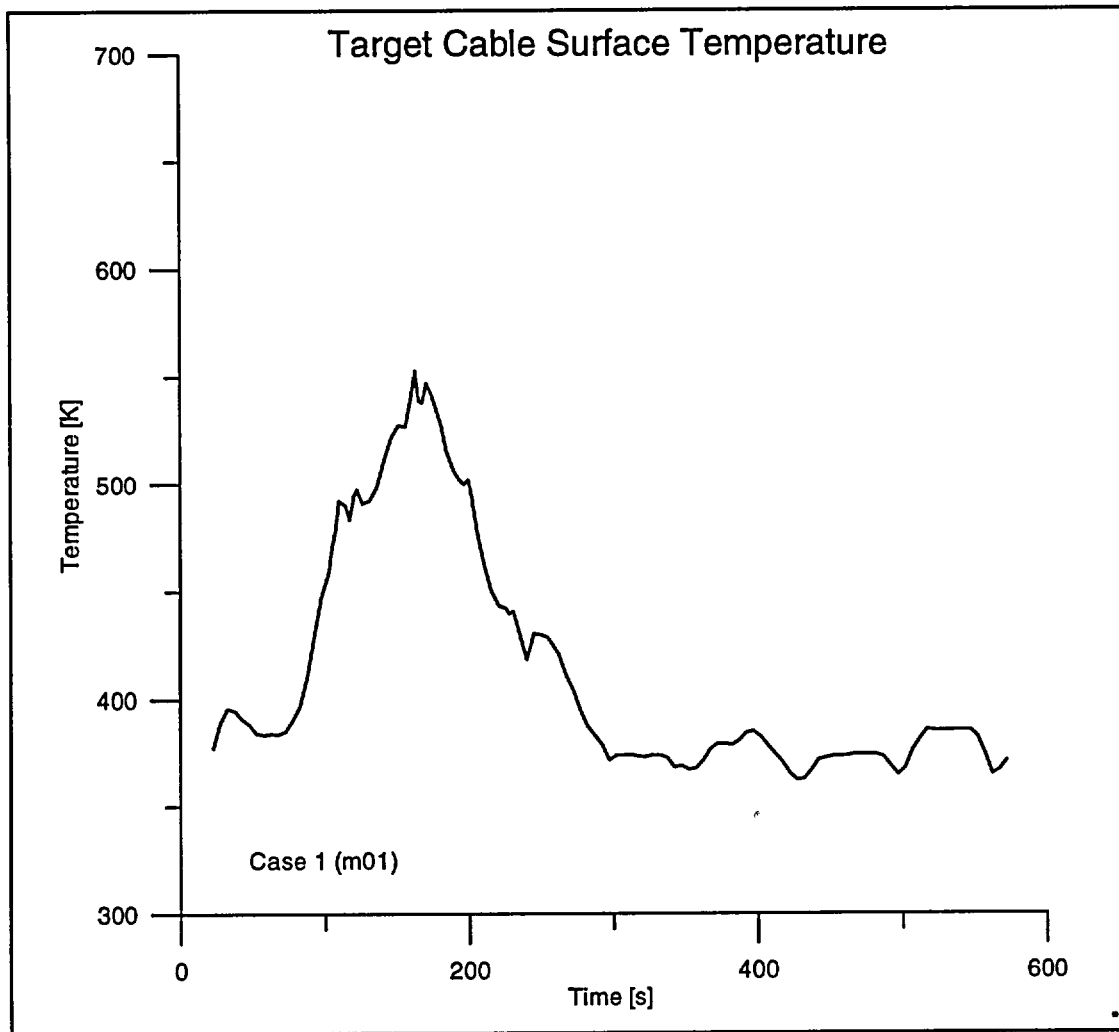


Fig. 12 Surface temperature over time for case 1

Cable Tray Fires of Redundant Safety Trains Benchmark Part I

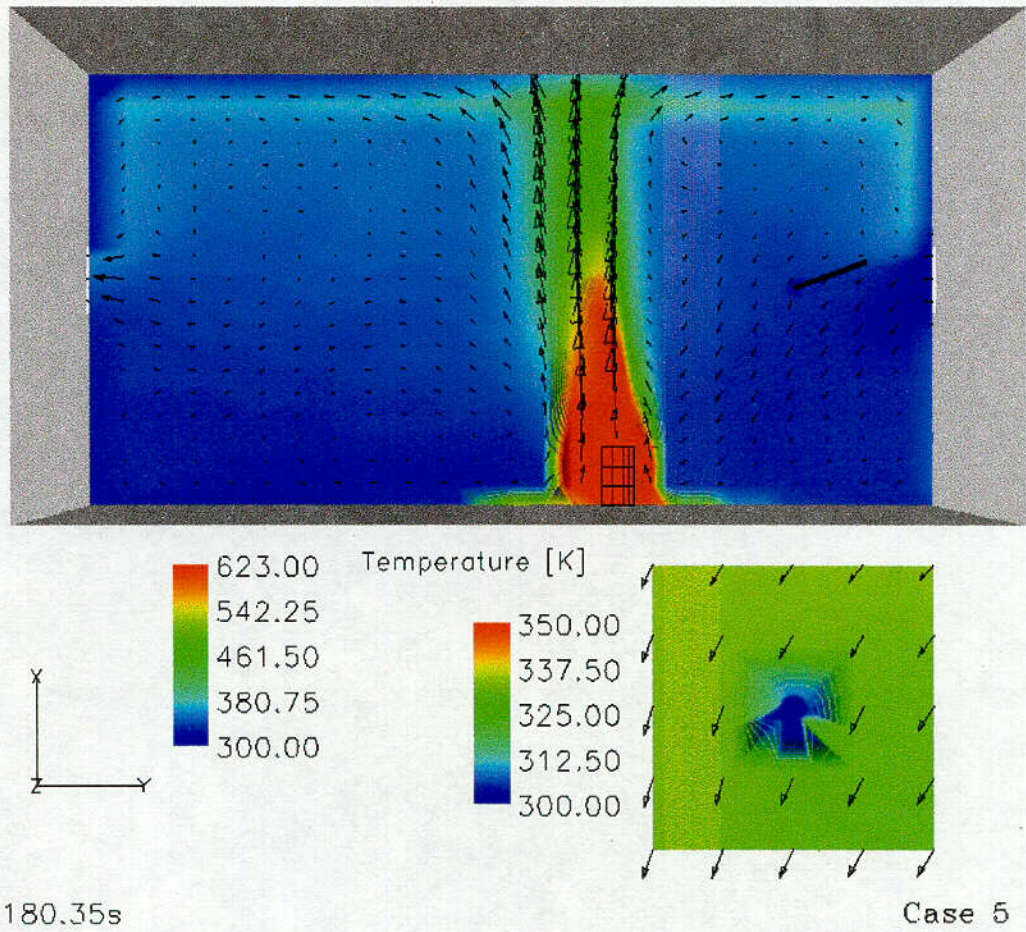


Fig. 13 Flow field in the fire room with ventilation system on (case 5)

C19
184

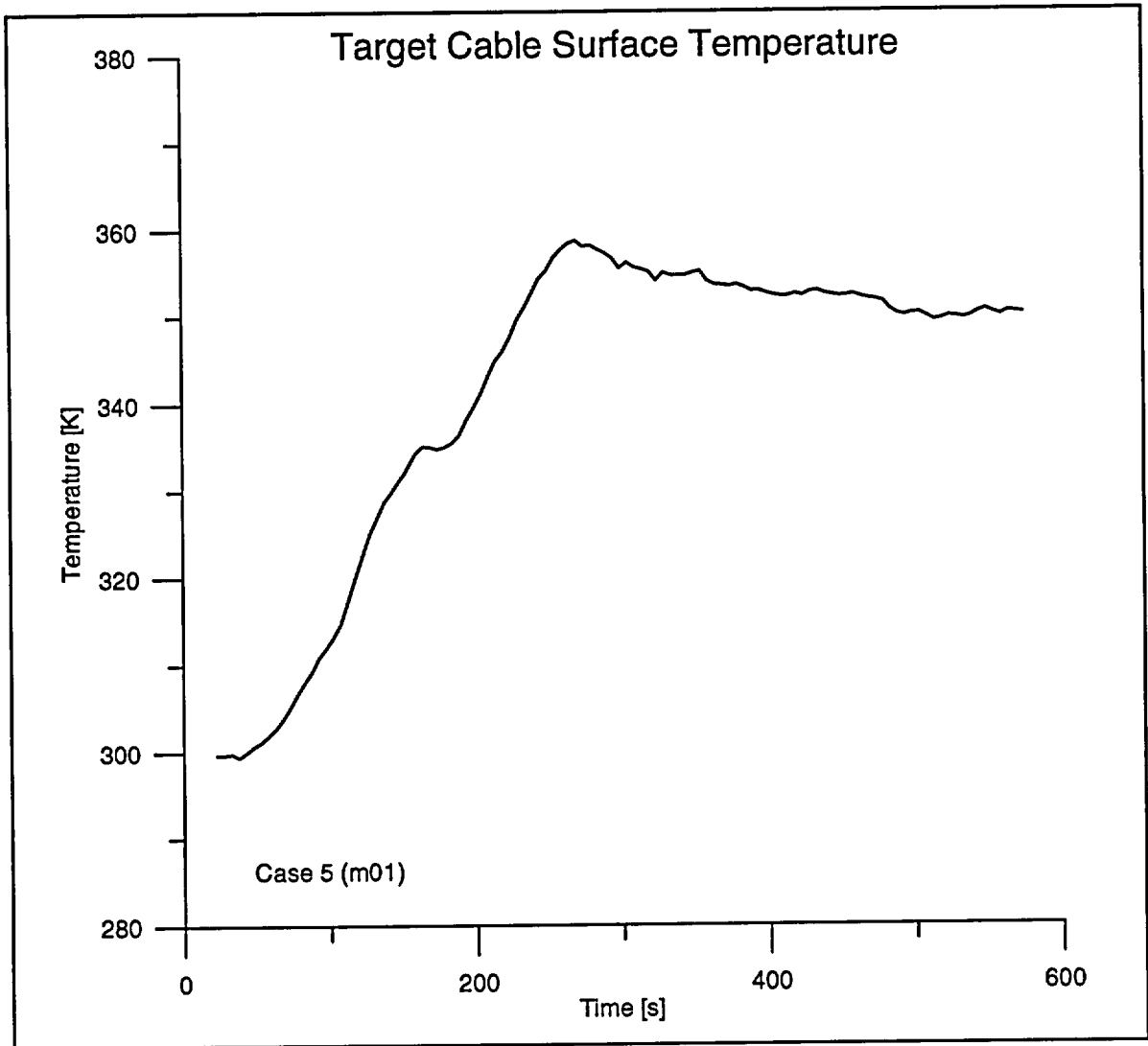


Fig. 14 Cable surface temperature with case 5

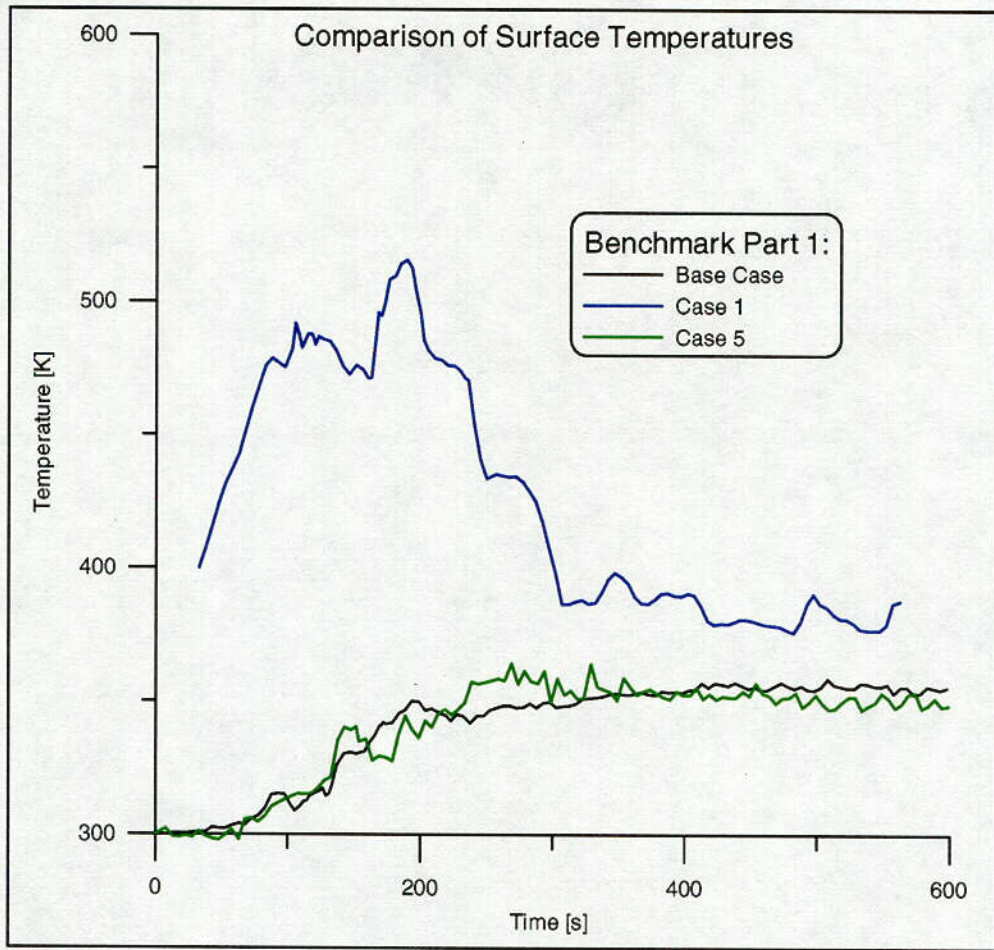


Fig. 15 Comparison of surface temperatures for benchmark part 1

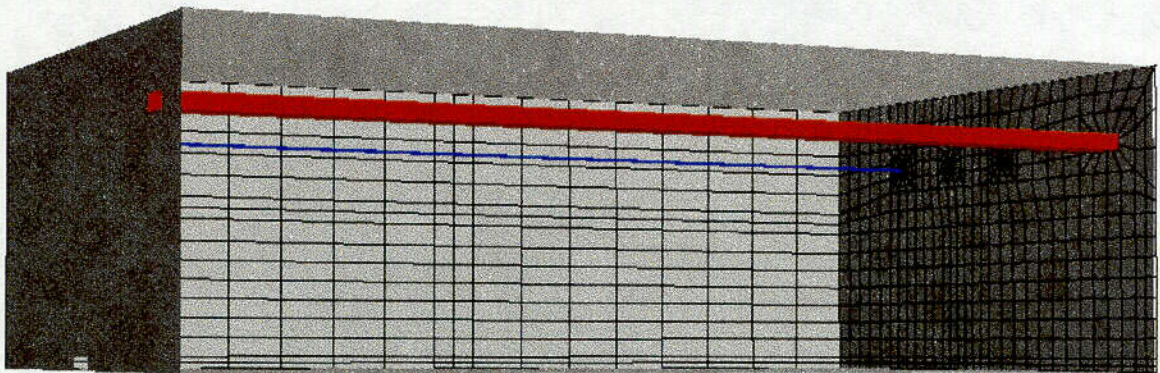


Fig. 16 CFX model for benchmark part 2

C20
186

Cable Tray Fires of Redundant Safety Trains Benchmark Part II

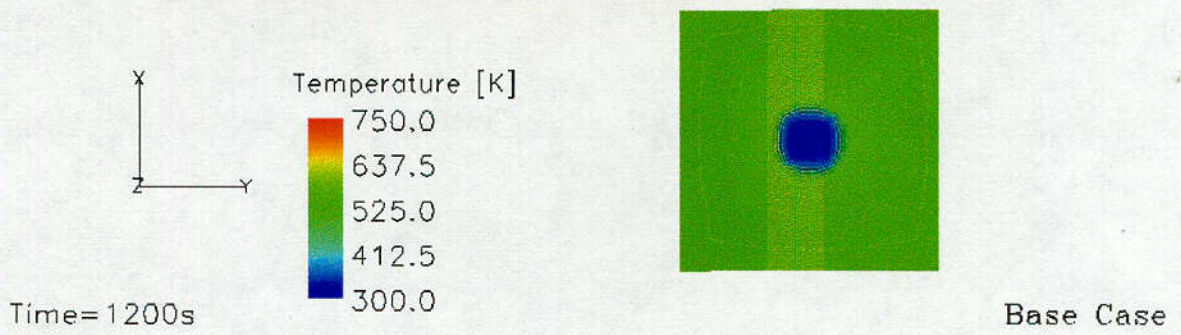
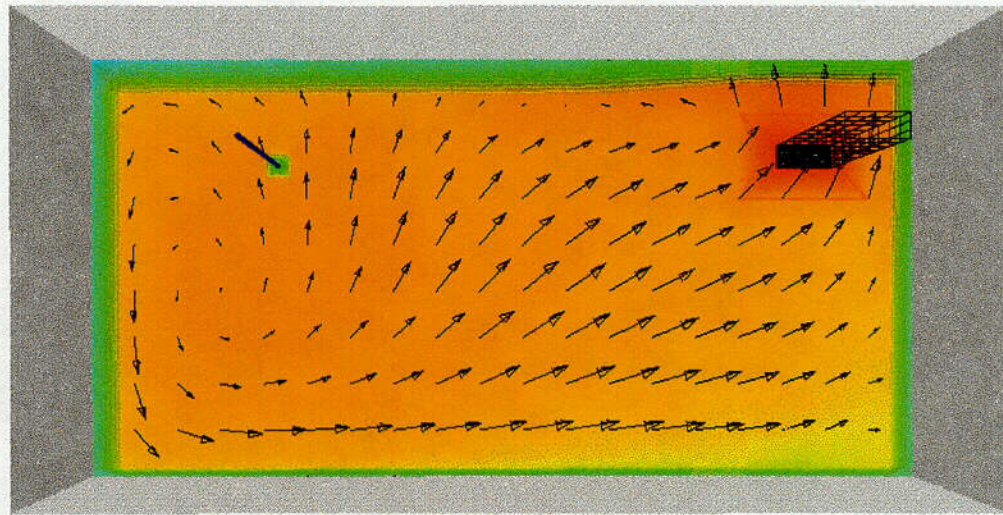


Fig. 17 Temperature distribution after 1200 s (base case)

C21
187

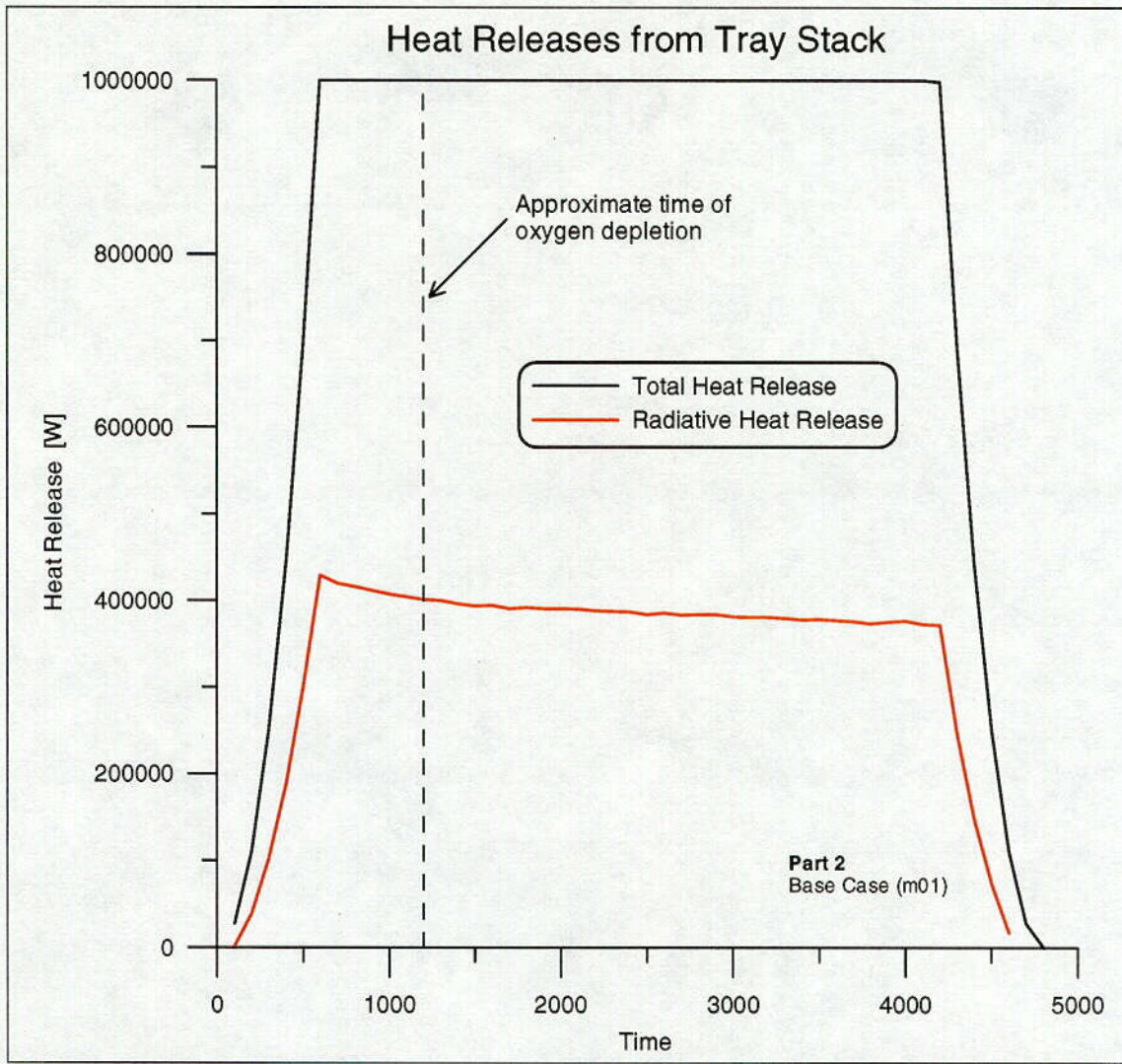


Fig. 18 Given heat release rate over time (part 2, base case)

C22
188

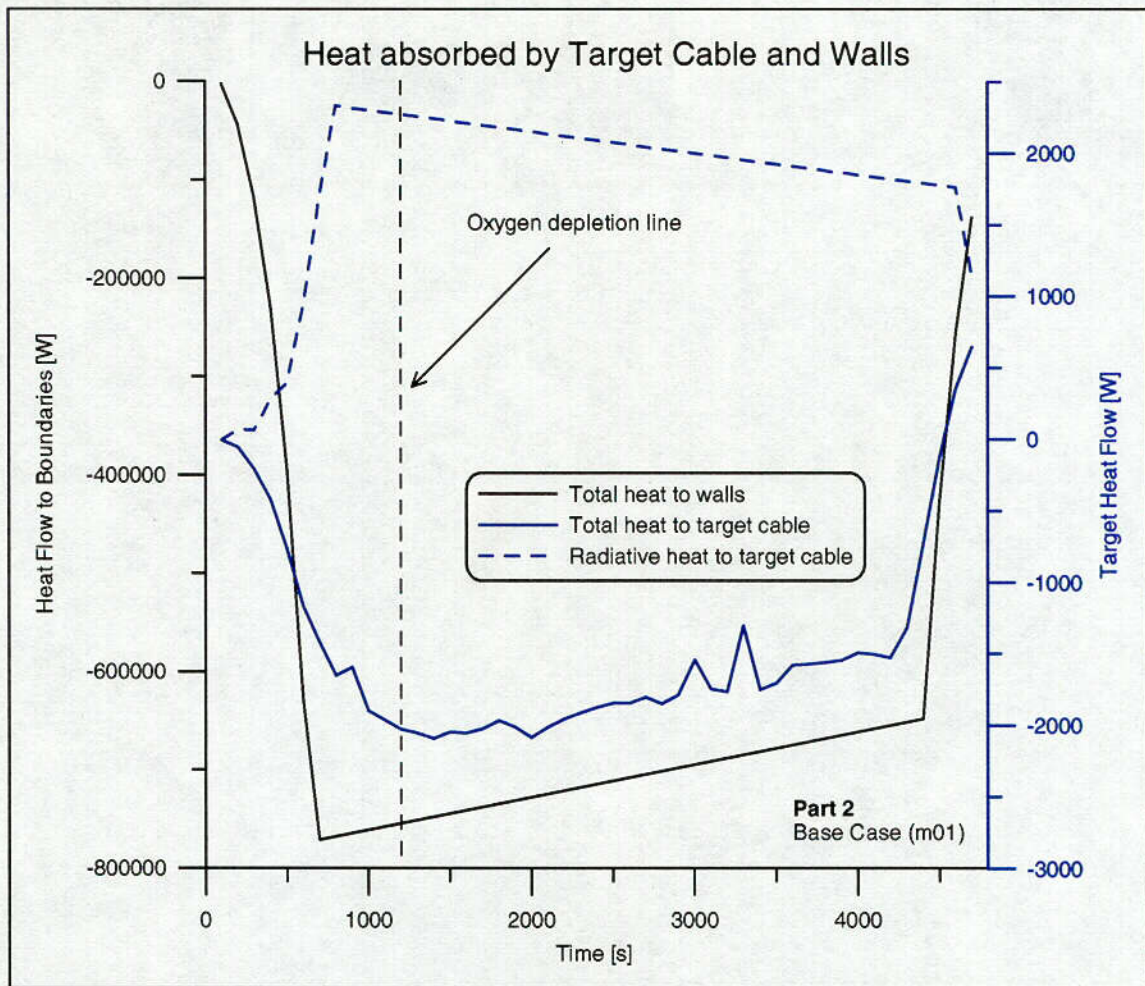


Fig. 19 Heat absorbed by the target cable (part 2, base case)

C23

189

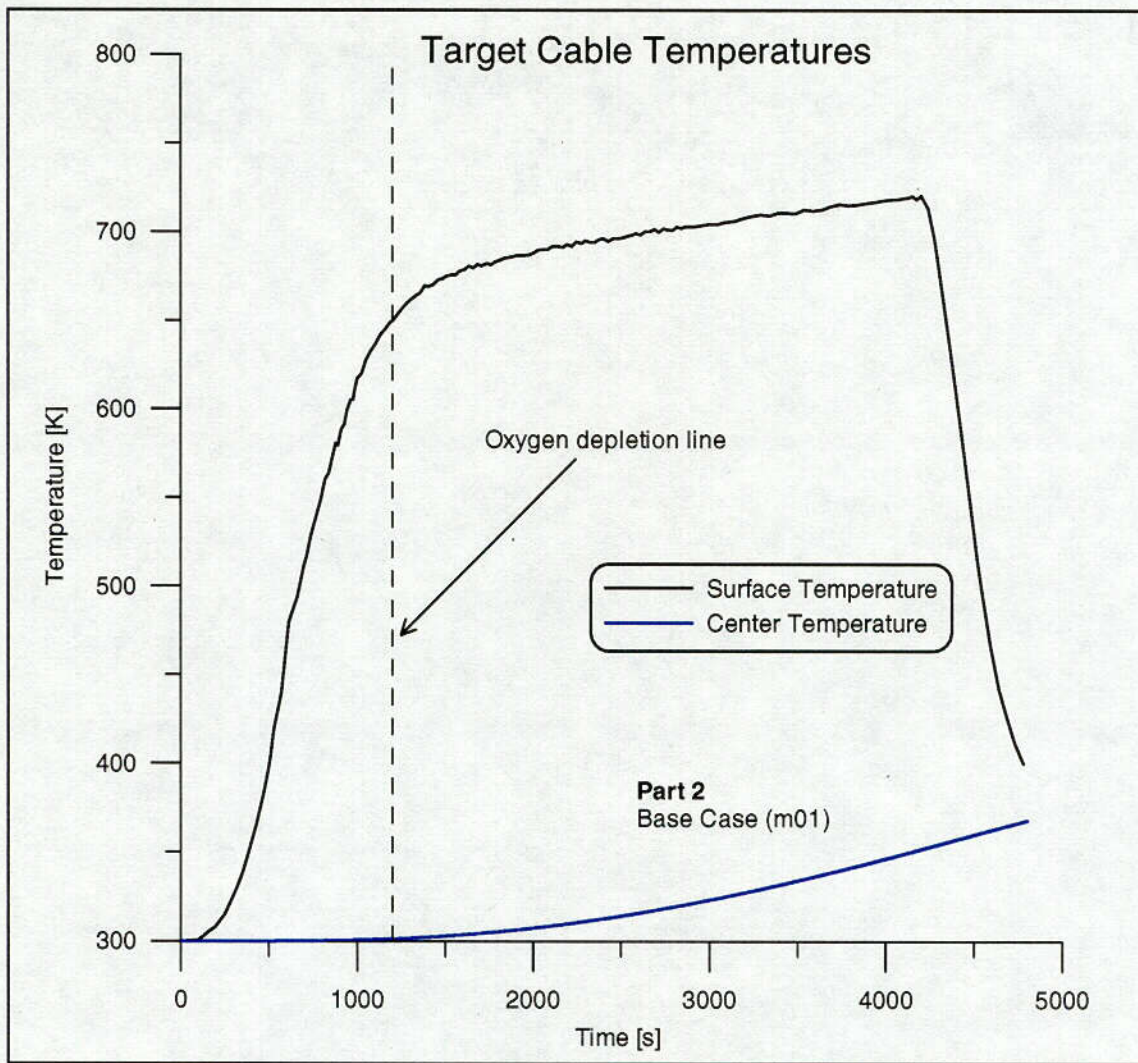
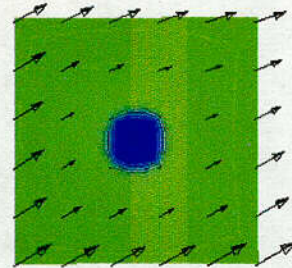
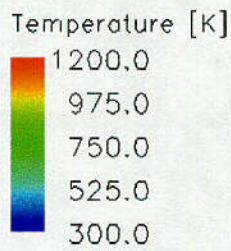
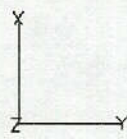
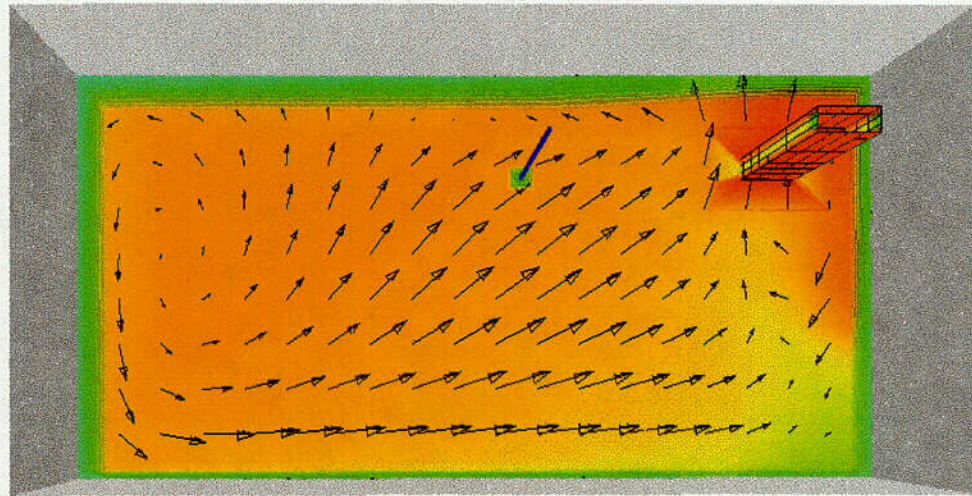


Fig. 20 Target cable temperatures during the base case of part 2

C24
190

Cable Tray Fires of Redundant Safety Trains Benchmark Part II



Time=700.25s

Case 6

Fig. 21 Temperature distribution after 700 s for case 6

C25
191

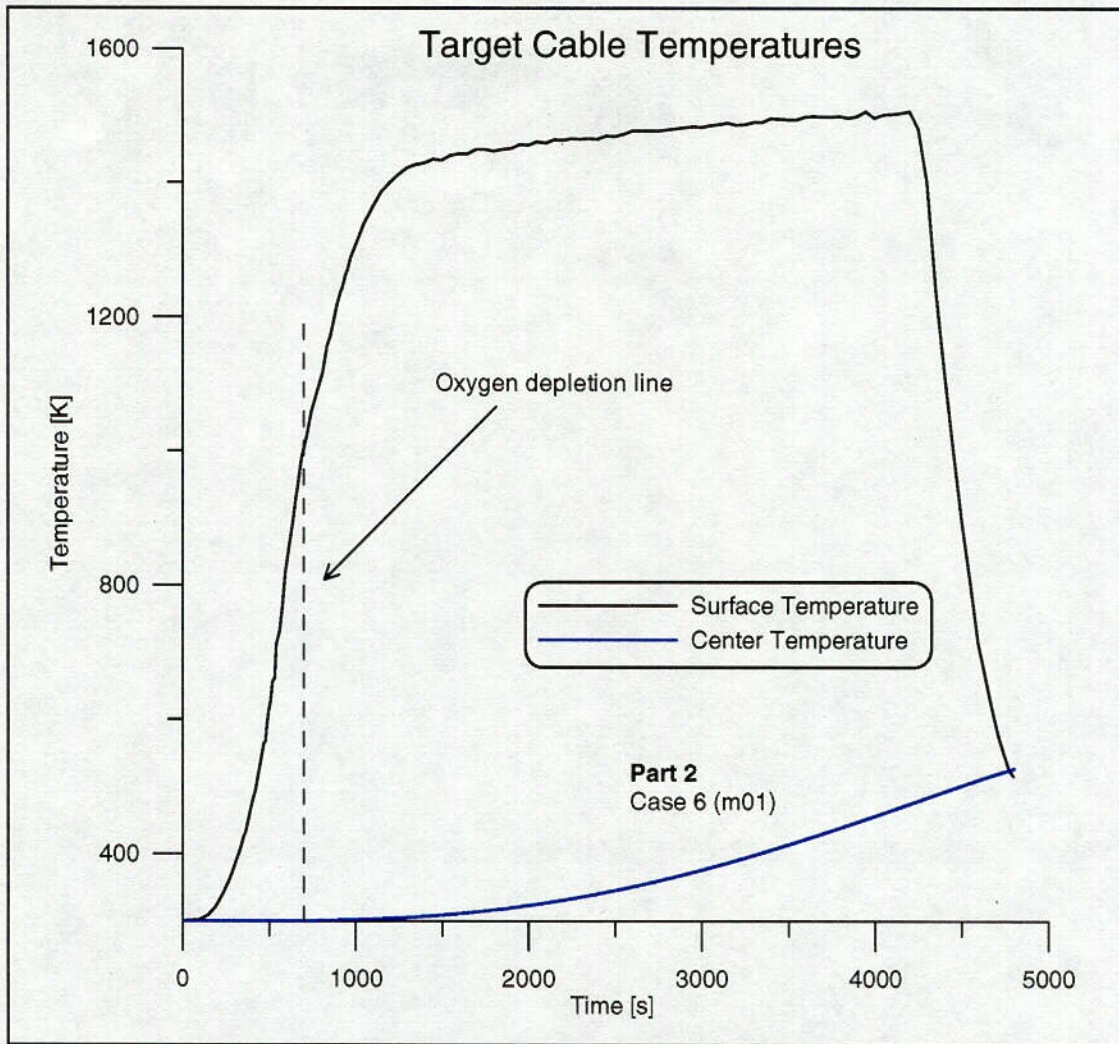


Fig. 22 Target cable temperatures for case 6

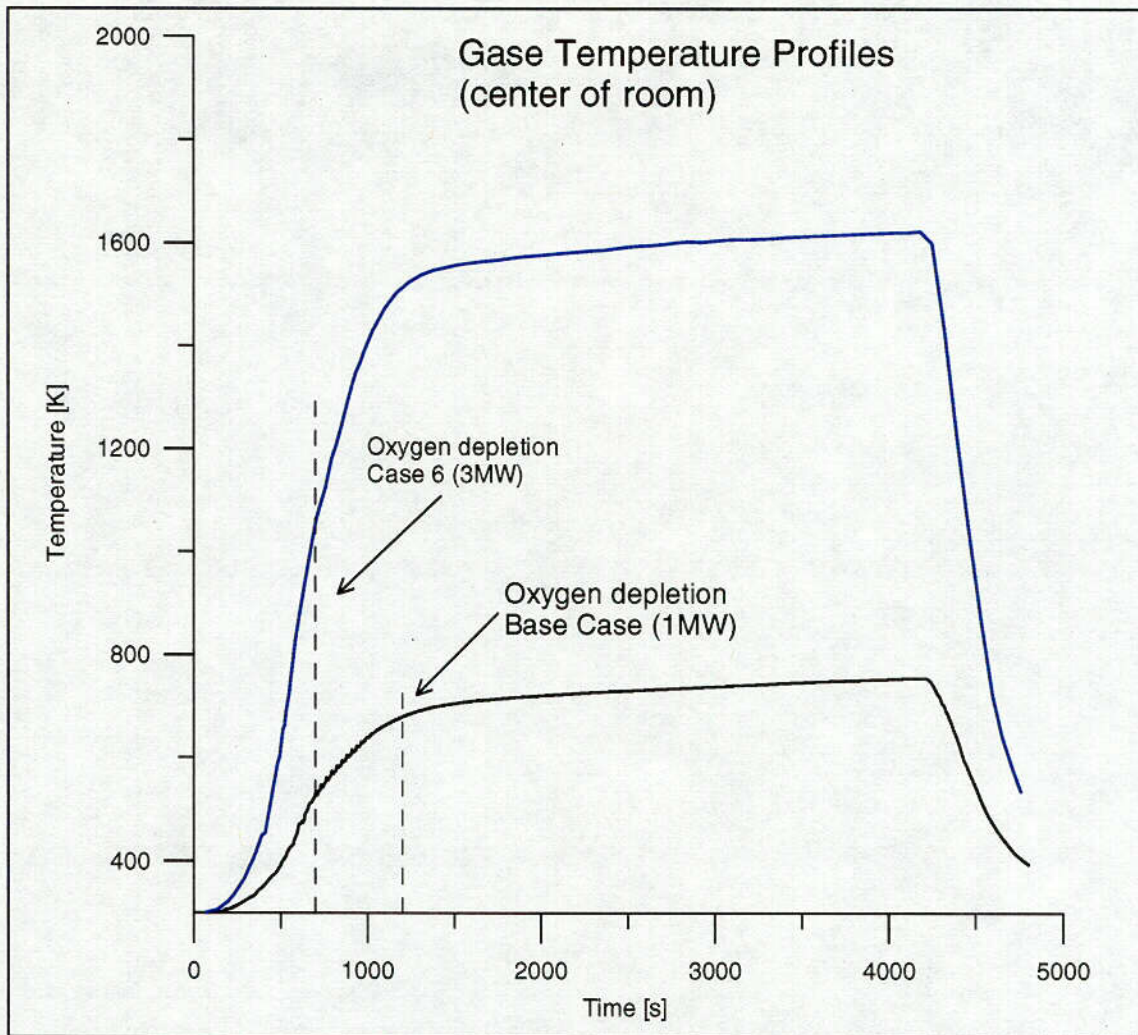


Fig. 23 Profile in the center of the room for base case and case 6

C27
 193

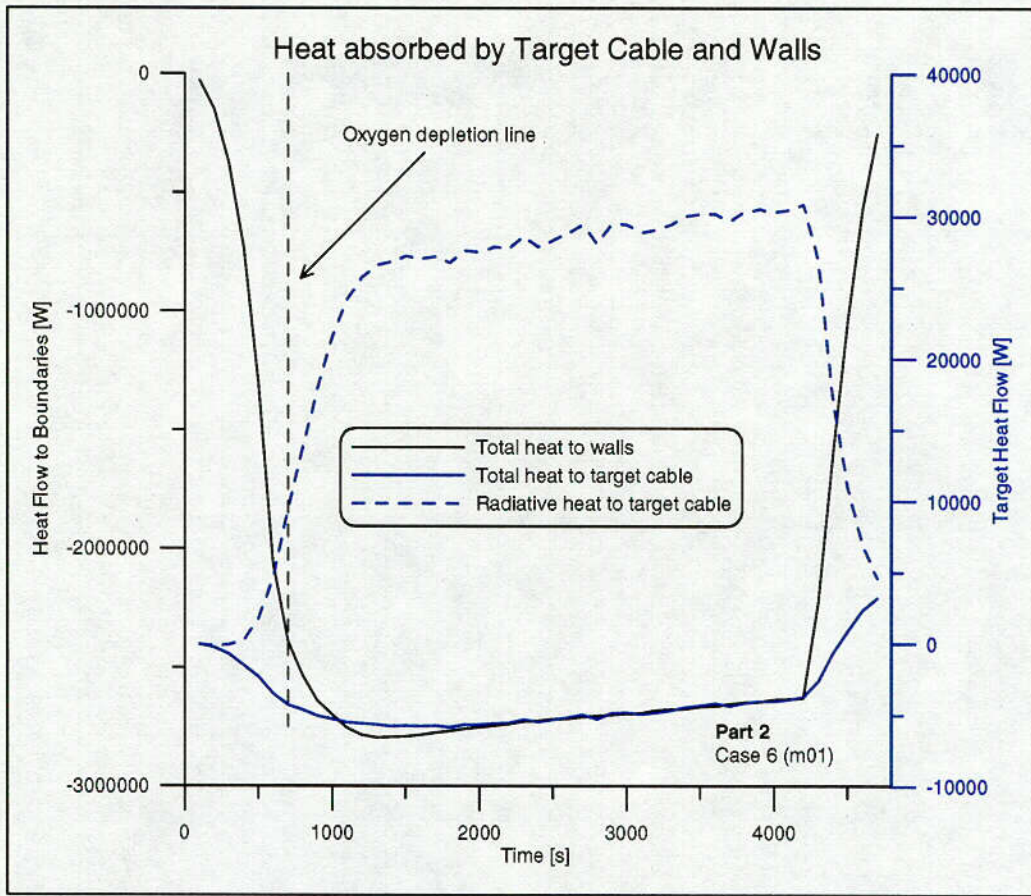
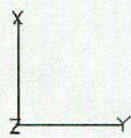
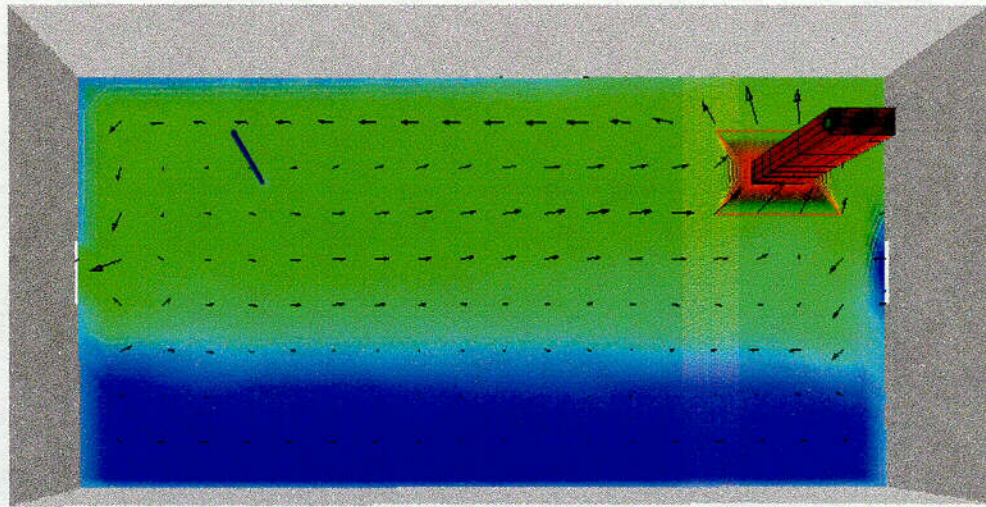
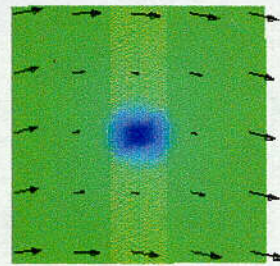
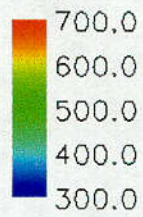


Fig. 24 Heat flows to walls and target cable for case 6

Cable Tray Fires of Redundant Safety Trains Benchmark Part II



Temperature [K]



Time=4200.25s

Case 10

Fig. 25 Temperature stratification after 4200 s for case 10

C29
195

Cable Tray Fires of Redundant Safety Trains Benchmark Part II

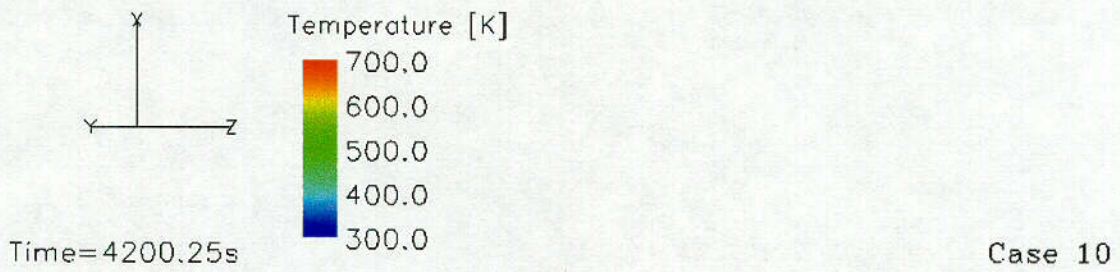
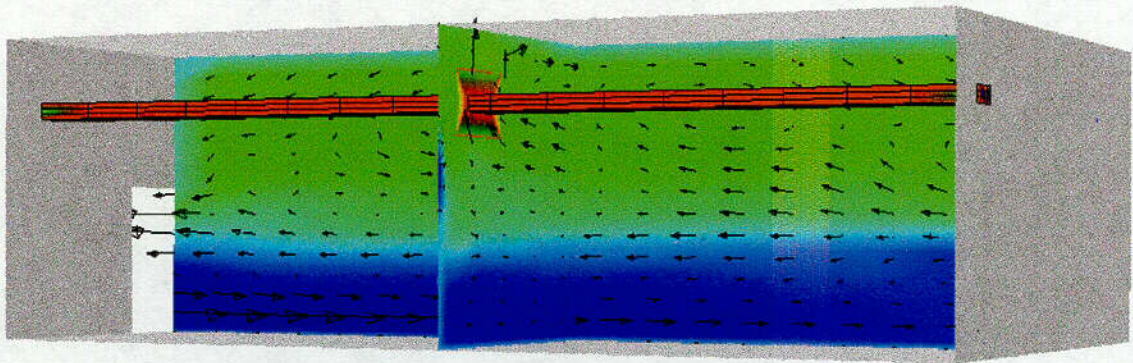


Fig. 26 Side view of the room at the end of the maximum power release

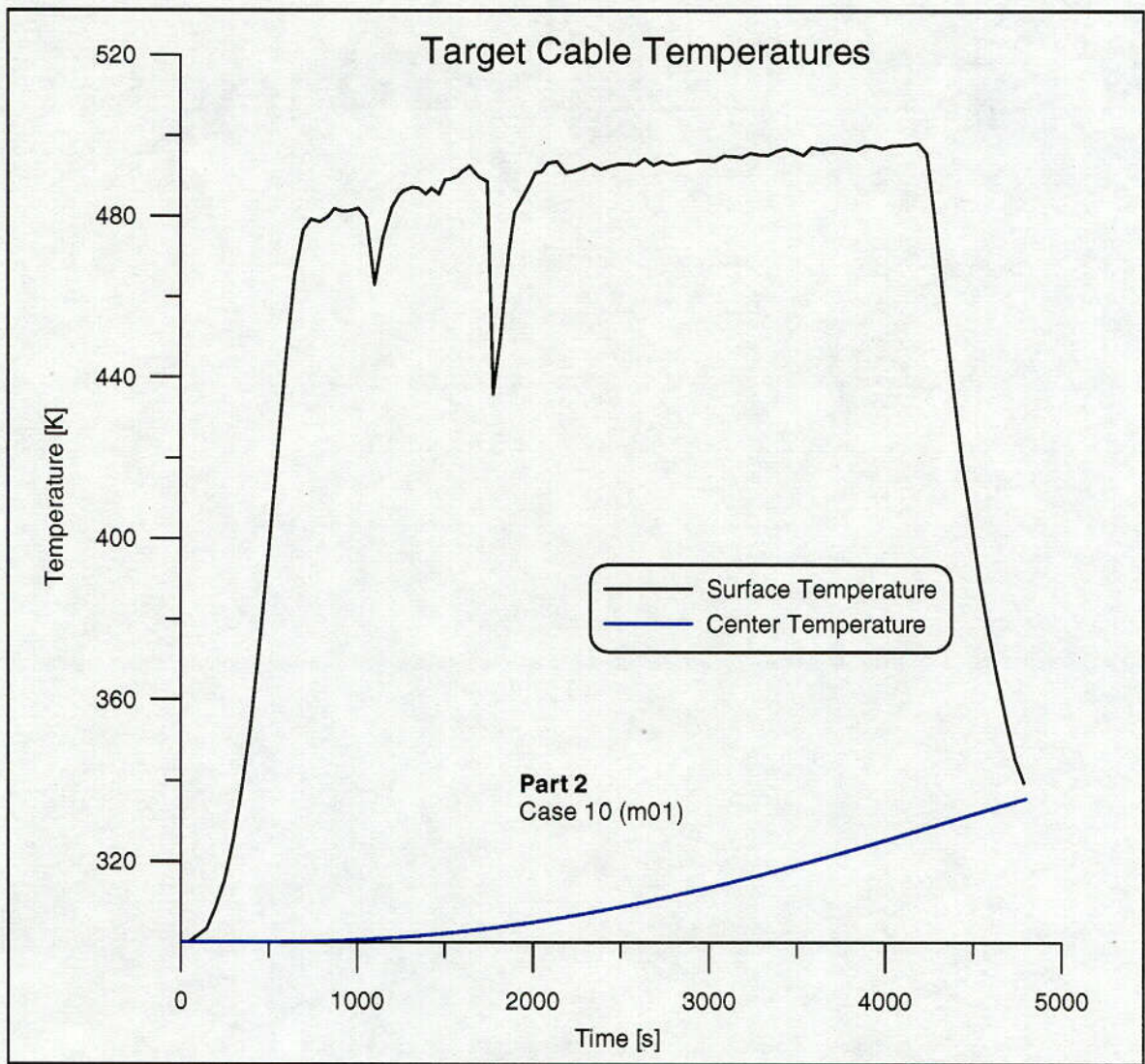


Fig. 27 Target temperatures over time for case 10

C31
197

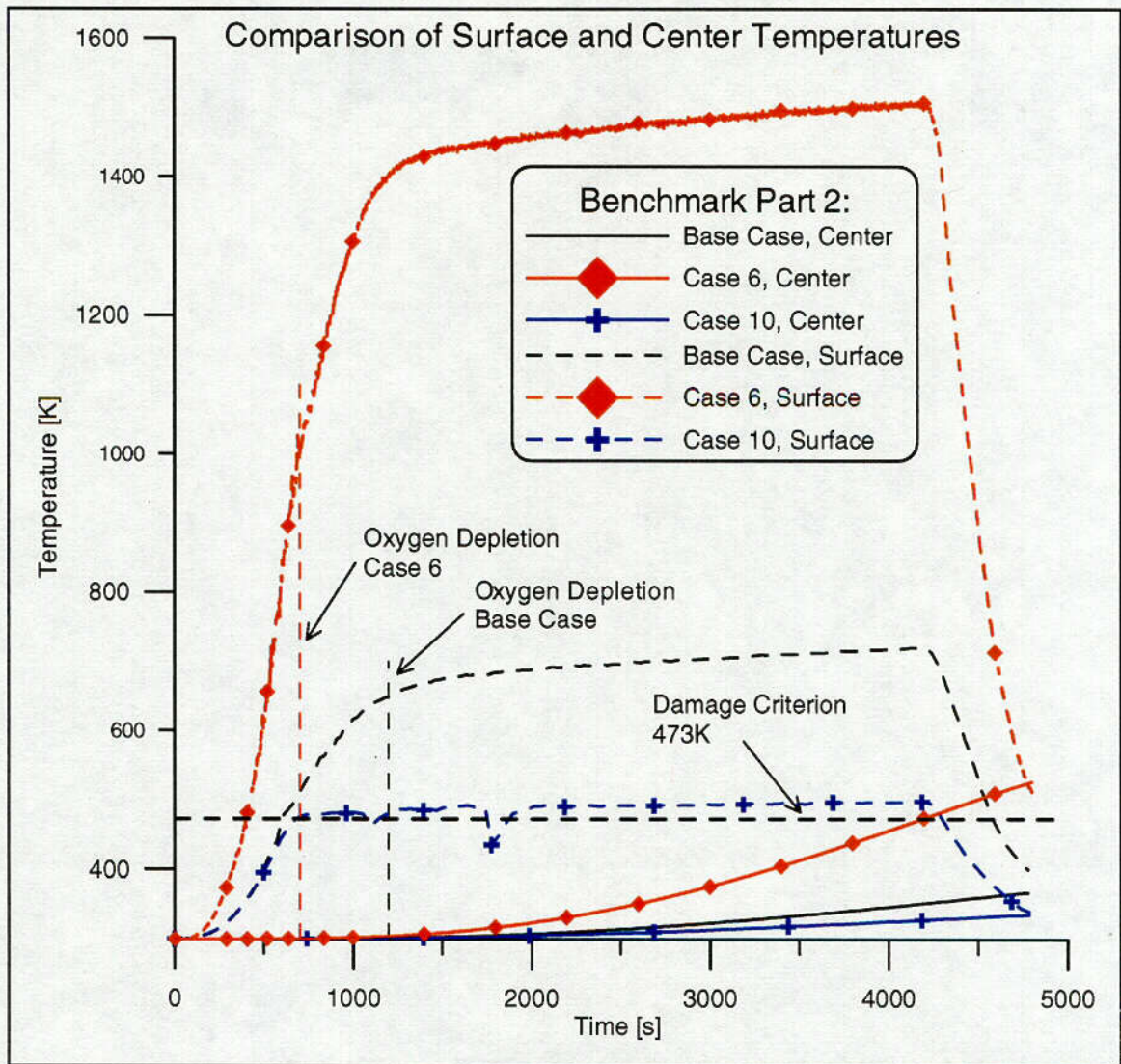


Fig. 28 Comparison of cable temperatures for base case, case 6 and case 10

C32

198

Tab. 1 Summary of results of simulations

	Max. UL Temp. [K]	Max. Flux on Target [W/m ²]	Max. Target CL Temp [K]
Part 1			
Base Case	360 (180s)	210	300
Case 1	360 (180s)	210	300
Case 5	350 (180s)	210	300
Part 2			
Base Case	680 (1200s)	840	301 (368)
Case 6	1065 (700s)	5800 (700s)	532(4800s)
Case 10	525 (4200s)	500	335

*109/2-1
1.1.1*